CHAPTER 12

Advances in Comprehensive Two-Dimensional Gas Chromatography (GC×GC)

CHRISTIANE EISERBECK,*[a] ROBERT K. NELSON,[b] CHRISTOPHER M. REDDY[b] AND KLITI GRICE[a]

[a] Curtin University, WA Organic and Isotope Geochemistry Centre, Department of Chemistry, GPO Box U1987, Perth, WA 6845, Australia; [b] Department of Marine Chemistry and Geochemistry, Woods Hole Oceanographic Institution, Woods Hole, MA 02543, USA
*Email: Christiane.eiserbeck@gmail.com

12.1 Introduction

Comprehensive two-dimensional (2D) gas chromatography (GC×GC) started to attract analytical chemists about 20 years ago. Liu and Phillips[1] reported the first comprehensive 2D GC analysis of an oil sample and the 2D contour plot drew further attention by the scientific community.

A number of reviews published in the past summarise the development of GC×GC in the earlier years up to 2008.[2–9] More recent reviews published in 2012[10,11] capture the functionalities and provide comprehensive summary and discussion of recent developments in modulator and detector technology. This chapter extends these reviews, focusing on the application of GC×GC to a broad range of disciplines in the geosciences.

GC×GC is the next development step after 2D separation using heart-cutting. While heart-cutting can only accomplish 2D separation in a narrow,

RSC Detection Science Series No. 4
Principles and Practice of Analytical Techniques in Geosciences
Edited by Kliti Grice

Published by the Royal Society of Chemistry, www.rsc.org

predetermined time window, GC×GC transfers all effluent from the primary column through to the secondary column, maximising the sample resolution throughout the entire analysis. Hence, it is called comprehensive 2D GC as opposed to the heart-cutting technique, because the complete sample is separated in two dimensions. GC×GC uses two orthogonal stationary phases (such as non-polar and polar) within one analysis, thus adding a second dimension of chromatographic resolution. A chromatographic plane is created by these two orthogonal separation mechanisms. The obtained enhancement of chromatographic resolution (compared to conventional GC) is created by the additional peak capacity within that plane. A third dimension of separation can be added to GC×GC when it is coupled with a time-of-flight mass spectrometer (TOF-MS).

The placement within that plane provides invaluable insights into unknown compounds with regards to their elution order within a certain compound class (for details see section 12.2.6) as well as basic chemical and physical properties.[12]

The power of GC×GC rests in its capability of high-resolution separation of very complex mixtures such as biological and geological samples.[6,13–17] Applications range from the fields of metabolomics, medical and pharmaceutical separation problems right to the geosciences including petroleum geochemistry. GC×GC has also significant applications emerging in mineral exploration (Grice, personal communication).

Geological samples such as crude oils, condensates, and rock extracts are mixtures of thousands of compounds from highly abundant straight-chain n-alkanes to polycyclic saturated, unsaturated, and aromatic hydrocarbons, diamondoids, metalloporphyrins, and polar compounds containing heteroatoms. These compounds can vary significantly in concentration, challenging conventional separation techniques. The enhanced resolving power of GC×GC makes it an ideal choice for analysis of these complex mixtures.[4,6,14,18–27] The expanded peak capacity allows for simultaneous analysis of saturated and aromatic hydrocarbons as well as more polar compounds containing heteroatoms such as oxygen, nitrogen and sulfur that are commonly present in fluids and rocks from the subsurface.

This chapter introduces the principles of GC×GC, describes recent technical developments, and discusses a selection of applications to demonstrate the capabilities of GC×GC and its value for the geosciences. A summary of reviews and applications of GC×GC in the field of geosciences is listed in Table 12.1.

12.2 Technical Background

12.2.1 Basic Principle

In GC×GC, two capillary GC columns are fitted in the GC oven, connected *via* a transfer line. Compounds eluting from the first column within a predefined time window (modulation time) are cryogenically trapped and

Table 12.1 Reviews and applications of GC×GC in the geosciences.

- Reviews on GC×GC analysis[2–7,10,11,28]
- Whole fluid analysis of very complex samples such as crude oils[8,18,19,29–35]
- Separation and characterisation of unresolved complex mixtures[14,17,23,36]
- Fingerprinting[22,24,26,27,37,38]
- Statistical methods applied to data processing and interpretation[22,39–41]
- Monitoring of gradual changes in biomarker composition of oil in the environment (*e.g.* oil weathering)[42–51]
- Fluid-source-correlation studies[16,47,52]
- Detailed studies of biomarker distribution in geological samples including diamondoids,[53–55] specific biomarkers such as 18α(H)- and 18β(H)-oleanane, lupane[27,56]
- Paleoenvironmental proxies[34,35]
- Pyrolysis-GC×GC[25,57]
- Study of nitrogen-containing biomarkers[58–60] and sulfur-containing compounds[25] in crude oil fractions
- Technical studies (*e.g.* modulators, peak shape,[61] retention time reproducibility)[62,63]

focused before transfer onto the second column. A secondary oven housing the subsequent column is situated inside the main oven for independent temperature control of the second-dimension separation.

The continuous modulation of the complete sample in one analysis makes this technique a comprehensive 2D GC. In contrast, earlier 2D separation techniques that used a heart cut to transfer effluents of only one single time window for secondary separation were very limited to a specific separation problem.

12.2.2 Instrument Setup

The most commonly used GC×GC system is the LECO Pegasus 4D GC×GC (LECO Corporation, St. Joseph, MI, USA) which has a flame ionisation detector (GC×GC-FID) or can be coupled to a time-of-flight mass spectrometer (GC×GC-TOF-MS). The Zoex system (Zoex Corporation, Houston, TX, USA) is another system that is often applied in the petroleum field.

Figure 12.1 shows a schematic of a typical setup of a GC×GC-TOF-MS instrument. An exhaustive review of the setup and discussion of the individual components of the GC×GC system was presented by Adahchour *et al.*[2–6]

12.2.2.1 Columns

The primary column, along with the dual-stage cryogenic modulator, resides in the main oven, whereas the second-dimension column is fitted in a separate oven, allowing for independent temperature control.

Especially for applications in geosciences, the most common column combination includes a polar and a non-polar stationary phase. The

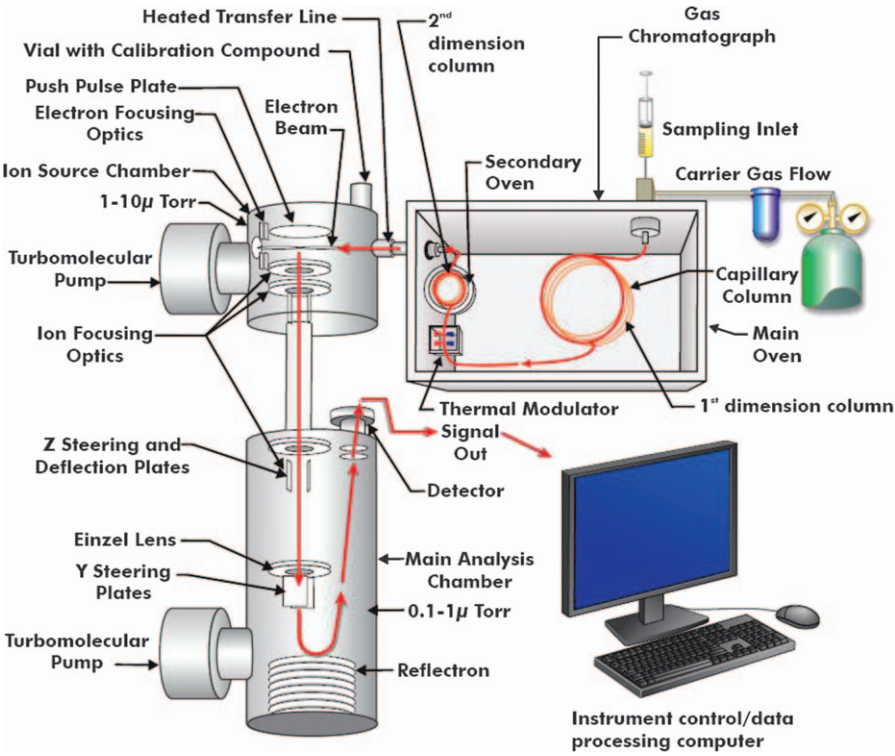

Figure 12.1 Schematic of a typical set-up of a GC×GC-TOFMS instrument (Source: LECO® website http://www.leco.com.au/files/sep_sci_pegasus_4d_gcxgc-tofms_209–183.pdf), reprinted with permission from Leco®).

first-dimension column is commonly a non-polar column (*e.g.* 100% dimethylpolysiloxane coated) of about 25–50 m length separating based on volatility. This setup allows for comparison with regular 1D GC analyses that are often performed on a DB-1 or equivalent column.

The subsequent second-dimension separation is commonly performed on a polar column (*e.g.* a 50% phenyl polysilphenylene-siloxane coated) of about 1.25–3 m in length. The fast second-dimension separation is practically isothermal with no boiling-point-contribution to this separation, thus the separation is orthogonal because retention is exclusively based on the specific interactions of each compound with the stationary phase.

A combination *vice versa* (polar/non-polar) is also often applied. This way the sample is separated based on polarity in the first separation step followed by a volatility separation. Examples of the effect of these column combinations on the elution order are shown in Figure 12.2.

The polar/non-polar configuration was reported to show better resolution for saturated hydrocarbons and might thus be better suited for samples with a higher concentration of these compound classes.[21] However, for a more holistic overview of a sample containing saturated, aromatic, and polar

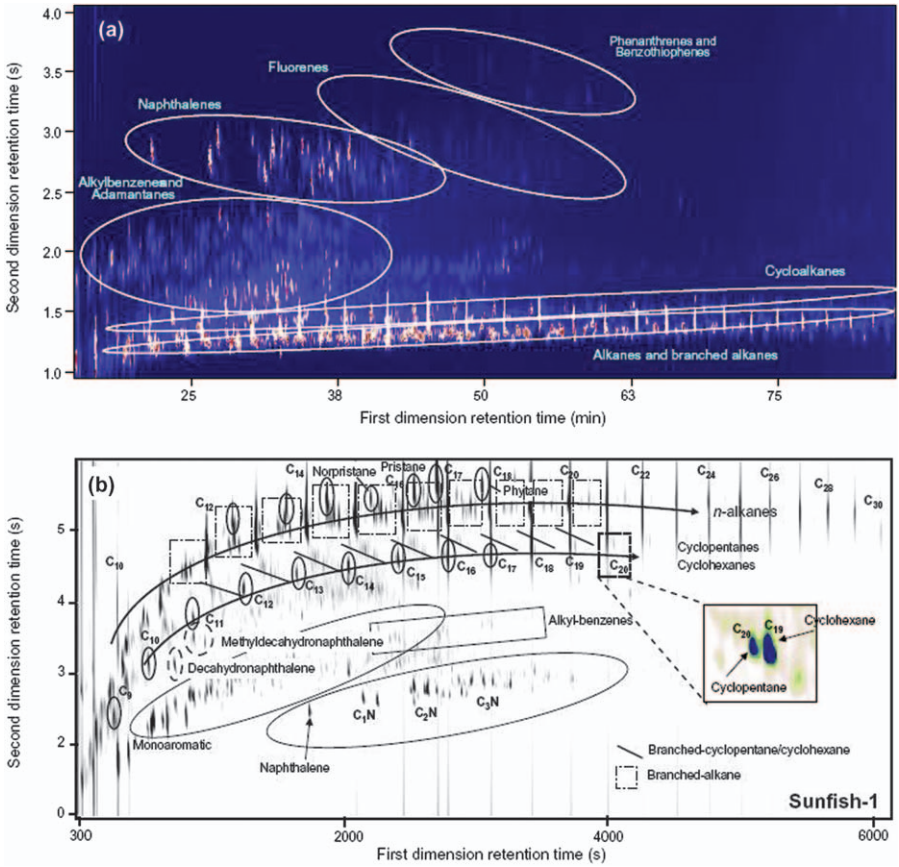

Figure 12.2 Exemplified elution pattern for the application of different column configurations: GC×GC analysis of land-plant oils. (a) GC×GC–FID plot of Sunfish-1 oil analysed using non-polar/polar column set. (b) GC×GC-TOFMS total ion chromatogram (TIC) of Sunfish-1 oil using polar/non-polar column set. b1, b2, and b3 display elution regions of alkanes/isoprenoids, alkylcyclopentanes/alkylcyclohexanes, and aromatics in 2D space, respectively.
Reprinted from Tran *et al.*,[14] Copyright (2010), with permission from Elsevier.

compounds, the non-polar/polar configuration is suggested and more applicable when comparing with 1D analyses.

Particularly in other disciplines such as medicine and metabolomics, non-orthogonal set-ups have been successfully applied. Enantioselective GC×GC of compounds in essential oils (*e.g.* tea tree oil, Chinese medicine) was achieved with both an orthogonal as well as a non-orthogonal approach.[6]

Depending on the separation problem at hand, a myriad of different combinations can be applied and the choice of the most suitable column combination is often the result of trial and error, particularly for very specific separation problems.

The length and diameter of the individual columns can also have an effect on the separation result, *e.g.* a wider internal diameter of the secondary column can extend the secondary retention time and thus increase the achieved separation. Alternatively, a secondary column with a reduced internal diameter can reduce the overall analysis time, which is usually long (*e.g.* 1.5–3 h) because of the slow temperature programme required to meet the modulation criteria.[6]

Overall, a large number of variables have to be taken into account when optimising the separation problem at hand such as the stationary phase, the column length, the column's internal diameter, the temperature programme, the modulation period. The separation success depends on the complex and sensitive interaction between these variables and often numerous attempts are required for optimised settings.

12.2.2.2 Modulator

The modulator is the crucial part in the separation system as it affects the separation and reproducibility. Modulators have developed significantly in the past decades. The most commonly used modulator is a thermal modulator consisting of a quad-jet system. It is placed between the two GC columns and creates two distinct trapping zones in which all effluents from the first column are cryogenically focused before thermal release onto the second column.

The dual-stage cryogenic modulator (*e.g.* LECO) operates with a cold and hot jet. The cold jet gas is dry nitrogen, chilled with liquid nitrogen. Alternatively, expanding liquid carbon dioxide is also used for cooling. The hot jet is operated with air that is heated to significantly higher temperatures than the column temperature, about 50 °C above the temperature of the main GC oven.

A more detailed summary of recent developments in modulator research was discussed by Marriott *et al.*[10] and Seeley.[11]

Modulation Period. The modulation period is the timespan during which eluents from the first separation step are trapped into bundles before they are released onto the second column.

The modulation period can affect the separation success significantly. The choice of the right modulation period for a particular separation depends on the nature of the hydrocarbon mix and the focus of the separation problem at hand. With longer modulation periods, more of the compounds that were separated on the first column are being mixed again in the modulator. For example, during a modulation period of 15 s all separated eluents from the first column are trapped and focused in a small band and injected together onto the second column as a mixture, losing the initial separation achieved in the first separation step. Therefore, the shortest possible modulation period is preferable.

However, this mixing effect needs to be balanced with the wrapping effect. Wrapping occurs when the modulation period is shorter than the time it takes all of the compounds that were transferred to the second column during the previous modulation phase to elute from the second column. If some compounds remain on the second column while the new set of compounds is being transferred onto the second column, these will overlap resulting in a false retention time as well as a misleading position within the chromatographic plane (see section 12.2.6). As an example, assume a modulation period of 5 s and a sample containing compounds which have a retention time of 7 s on the second column. In this case, these compounds will not elute during their modulation period of 5 s but will be carried over into the next modulation period and will elute after 2 s of that modulation period. They will therefore appear to have a retention time of 2 s and elute in a chromatographic space of less-retained compounds, *e.g.* high molecular weight aromatic compounds might elute together with n-alkanes and confuse the interpretation.

This is particularly relevant for unknown compounds, which in case of wrapping would elute in the chromatographic space of a different compound class from what they really are (see section 12.2.6). Furthermore, the separation of the following compounds will be compromised when there are compounds remaining on the column, and retention time shifts might be observed.

In summary, the preferred modulation time should be the minimum time (allowing for the most effective first-dimension separation) that is longer than the maximum secondary retention time of any compound in the sample. Commonly, modulation periods range from 5 to 10 s.

Another aspect that is affected by the modulation period is the peak width and shape. Compounds in high abundance have a larger peak with a broader peak width. If the peak width exceeds the modulation period, the compound will elute in two (or three) consecutive modulation periods, which can affect the peak shape as well as the automated interpretation, as the software might not recognise the two eluting parts as the same compound. In this case the peaks can be manually defined as the same compound.

12.2.2.3 Detector

The most commonly applied detector systems coupled to a GC×GC are the flame ionisation detector (FID) and the TOF-MS. Although double-focusing sector, quadrupole, and ion traps are popular MS detectors for GC, they have limited use in GC×GC because of their relatively slow scanning rates, compared to fast acquisition TOF-MS, better suited to characterise very narrow 2D peaks.

We do not go into detail about the technical background of these detectors here because they are widely used and a detailed description is not the focus of this chapter. A discussion of TOF-MS in general and in particular TOF-SIMS is given in Chapter 5 of this volume.

The FID is a very fast detector with high sensitivity. It allows for a precise quantification of individual compounds because it detects the compound and not just individual masses. Correct quantification requires a known retention time for the compound(s) of interest as well as baseline separation for each peak, which can often be challenging. The disadvantage of the FID is the lack of mass spectra and ion chromatograms to support compound identification.

TOF-MS, on the other hand, is equally fast and adds a third dimension of separation by obtaining mass spectra which allow for the use of ion chromatograms. Accurate identification of compounds, even unknowns, is possible *via* retention times and mass spectra. The study of series of *e.g.* diagenetic products is possible by using ion chromatograms.

TOF-MS is slightly less sensitive than FID and parameters such as the acquisition rate can have an effect on the separation result because it determines the signal-to-noise ratio. However, a high acquisition rate produces large data files which are challenging to handle afterwards. Again, this is a parameter that needs to be adjusted to the requirements of the separation problem.

TOF-MS operates at a push pulse rate of 5 kHz. This allows sufficient signal averaging time to ensure good signal-to-noise ratios while maintaining a data acquisition rate that is high enough to ensure accurate processing (signal average) of spectra for peaks eluting from the second-dimension column with second-dimension peak widths in the order of 50–200 ms at their base. Such narrow peaks require a high data acquisition rate. Hence, TOF-MS which can acquire data at up to 500 spectra per second, is the only mass spectrometer that can meet these requirements.

The sulfur chemiluminescence detector (SCD) has also successfully been used in combination with a GC×GC system to distinguish different sulfur-containing compound classes in the 2D space of a GC×GC, such as mercaptans, sulfides, thiophenes, benzothiophenes, dibenzothiophenes,[25] and thiodiamondoids.

FID *vs.* TOF-MS – Which to Choose? GC×GC-TOF-MS and GC×GC-FID complement each other and the use of both systems is recommended. GC×GC-FID results in an improved peak shape, reproducibility, and quantitative peak areas, while GC×GC-TOF-MS analysis provides high-resolution separation with access to full mass spectra throughout the chromatogram. GC×GC-FID is better suited for quantification of compounds.

Peak identification is more challenging in FID due to the lack of mass spectra for confirmation. However, once the retention times (first and second order) are established for a given compound of interest, ideally by repeat analysis of standards, peak volumes are best determined using the FID detector. The advantage of GC×GC-FID compared to the TOF-MS is the reproducibility, increased sensitivity ($\sim$5 times), quantitative detection of peak abundances, and improved peak shape.[27,56] Similar response factors

for all hydrocarbons in a GC×GC-FID chromatogram improve the comparability of obtained concentrations. Analysis of a whole oil results in a complete inventory of all GC-amendable compounds which is very powerful, due to the response factor of near unity.

A very simple advantage of GC×GC-FID is the lower maintenance cost, which allows for more affordable instrument settings with regard to separation problems that might require multiple analyses for an optimised result.

Furthermore, retention time stability is better in GC×GC-FID analyses. Retention time reproducibility was studied by Shellie *et al.*[62,63] Standard deviations of retention times (RT) in a run-to-run comparison based on 43 compounds in 6 consecutive runs were found to be on average 0.12% relative standard deviation (RSD) in the first dimension and 0.74% RSD in the second dimension. RT obtained on consecutive days were slightly less stable, although this was true mainly for very abundant compounds while RT of trace, minor, and intermediate concentration components were extremely reproducible. These RSD values represent ideal values obtained in very controlled conditions. Most applications of RT comparisons will require RT stability of compounds in different samples and in these cases the matter becomes more complex. Varying types of organic matter contain changing matrices for a particular compound that is to be compared which can result in slight changes in RT. Higher concentrations of one compound can also lead to elution in two separate modulation periods compared to low- to medium-abundance compounds which mostly elute within only one modulation period (depending on the peak width in relation to the chosen modulation period). Elution in multiple modulation periods can cause a slight shift in RT, depending on the point where the data processing software sets the peak maximum.

Eiserbeck *et al.*[27] determined the RT stability for multiple GC×GC-FID and GC×GC-TOF-MS analyses of 17α,21β(H)-C_{30}-hopane in seven different crude oil samples with varying 17α,21β(H)-C_{30}-hopane (hopane) concentrations. The GC×GC-FID measurements had a RSD of 0.05% and 0.54% for first and second RT compared to 0.16% and 1.82% for GC×GC-TOF-MS. The higher RSD compared to the results obtained by Shellie *et al.* are partly due to the varying matrices present in seven different oil samples compared to one single sample that was studied by Shellie *et al.*[62] Furthermore, Eiserbeck *et al.*[27] observed compounds coeluting with hopane in some of the analysed oil samples which were partially resolved in the second dimension, obscuring the true second dimension RT of 17α,21β(H)-C_{30}-hopane.

GC×GC-quadrupole MS and GC×GC-combustion isotope ratio mass spectrometry (GC×GC-irMS) have been employed in other disciplines such as drug screening or characterisation of essential oils; however, these detection techniques operate at lower acquisition rates (~20–25 Hz) and thus lose resolution capability of GC×GC (see Marriott *et al.*[10] and references therein). Nonetheless, GC×GC-quadrupole MS has been successfully applied to hydrocarbon mixtures in the past.[19] Developments towards more rapid acquisition rates up to 50 Hz for GC×GC-quadrupole MS are under way

for scan and single-ion monitoring (SIM) mode (290 amu mass range, 40–330 *m/z*).[64,65]

GC×GC-TOF-MS is pre-eminent for detailed biomarker studies. The obtained mass spectra add a third dimension of separation which is required for identification of coeluting or unknown compounds. Selected ion chromatograms can provide invaluable information in areas of high peak density.

12.2.3 Sample Preparation

Because of the enhanced peak capacity of GC×GC, no sample separation is required before the analysis. The whole sample is diluted in hexane or similar solvents and analysed simultaneously. Separation of asphaltenes might be performed if required, using a centrifuge, to prevent blocking of the capillary column.

With whole fluid injection, saturated, aromatic, and polar compounds can be studied in one chromatogram without loss of resolution. Furthermore, potential losses of the more volatile, low-molecular-weight compounds during preparation of the sample as previously necessary (such as liquid chromatography) are reduced. Moreover, the risk of introducing contamination to a geological sample during sample preparation is also reduced. This can be particularly valuable in studies of early life in which the first appearance of compounds indicating living organisms, such as steranes, is the key question and the presence of such compounds in the sample due to contamination would be misleading and render the sample invalid.

Furthermore, some unsaturated compounds are thermally unstable or prone to rearrangement when treated with *e.g.* molecular sieves (see section 12.4.2.2). GC×GC separates these samples chromatographically without any prior wet chemical treatment and thus maintains the natural composition. Similarly, argentation chromatography of non-polar fractions obtained from liquid chromatography into saturated and unsaturated compounds can result in rearrangements of double bonds in olefins. None of these preseparation steps is necessary for GC×GC analysis, making it a valuable tool for analysis of unstable compounds.

However, for a specific, known separation problem that might be limited to only a certain number of compounds that are not at risk of rearrangement, fractionating the sample before analysis is recommended as this will simplify the chromatogram, allow more chromatographic space to separate particular compound classes without concern for 'wrapping' (see section 12.2.2.2)[17] and thus improve the interpretation as well as preserve the injector and capillary columns.

Pyrolysis-GC×GC is an alternative for sample injection of less accessible hydrocarbons in asphaltenes (see section 12.2.4). Furthermore, hydrous pyrolysis (HyPy, see Chapter 6) can be applied before GC×GC to obtain a GC-amendable sample.

12.2.4 Injector Methods Coupled with GC×GC

Wang *et al.*[25] first described the coupling of pyrolysis to GC×GC-FID and its application to the characterisation of petroleum source rocks. This study was extended by Payeur *et al.*[57] who evaluated the use of pyrolysis-GC×GC-TOF-MS to analyse the pyrolysis products of six whole-sediment samples from above, within, and below an organic carbon-rich Quaternary sapropel layer from the Mediterranean.

Valentine *et al.*[66] applied pyrolysis-GC×GC-TOF-MS to study the composition and source of asphalt volcanoes in the Santa Barbara Basin, off the coast of California, USA.

The combination of whole-sediment pyrolysis and GC×GC-TOF-MS is promising but the success is sensitive to the careful selection of the multiple analytical parameters, particularly the pyrolysis temperature and the operational temperatures and flow rates of the GC columns.

12.2.5 Data Processing

12.2.5.1 Signal Deconvolution in ChromaTOF® Software

The use of a TOF-MS ensures spectral continuity, thus allowing mass spectral deconvolution of coeluting peaks if these are characterised by different fragmentation patterns. The requirements for successful deconvolution are for the peak apexes of coeluting analytes to be at least separated by three scans and to differ somewhat in their mass spectra. This capability allows the identification of different coeluting compounds. The use of deconvoluted ion current (DIC) acts like a fourth dimension to the separation system. The ChromaTOF® GC software includes an automated signal deconvolution which can be added to the analysis sequence to produce extracted mass spectra free of interfering signals.

12.2.6 GC×GC Chromatogram—A Map for Biomarkers

GC×GC chromatograms are commonly displayed as contour plots (plan view, Figure 12.3), but can also be presented as mountain plots (see Figure 12.5c). In GC×GC chromatograms, compound classes are separated across the 2D plane spanned by the first and second dimension (Figure 12.3) according to their increasing volatility (non-polar column, first dimension) and polarity (polar column, second dimension).[24] With this sequence of capillary columns, the general elution order with increasing second-dimension retention time can be summarised as: n-alkanes < regular isoprenoids < irregular isoprenoids < alkylcyclopentanes < alkylcyclohexanes < bicyclic terpenoids < alkylbenzenes (Figure 12.3). Cyclic saturated compounds such as terpenoids elute further up in the first dimension and also slightly later in second dimension with each additional ring in the structure. Cyclic compounds (including mono- and diunsaturated compounds) elute

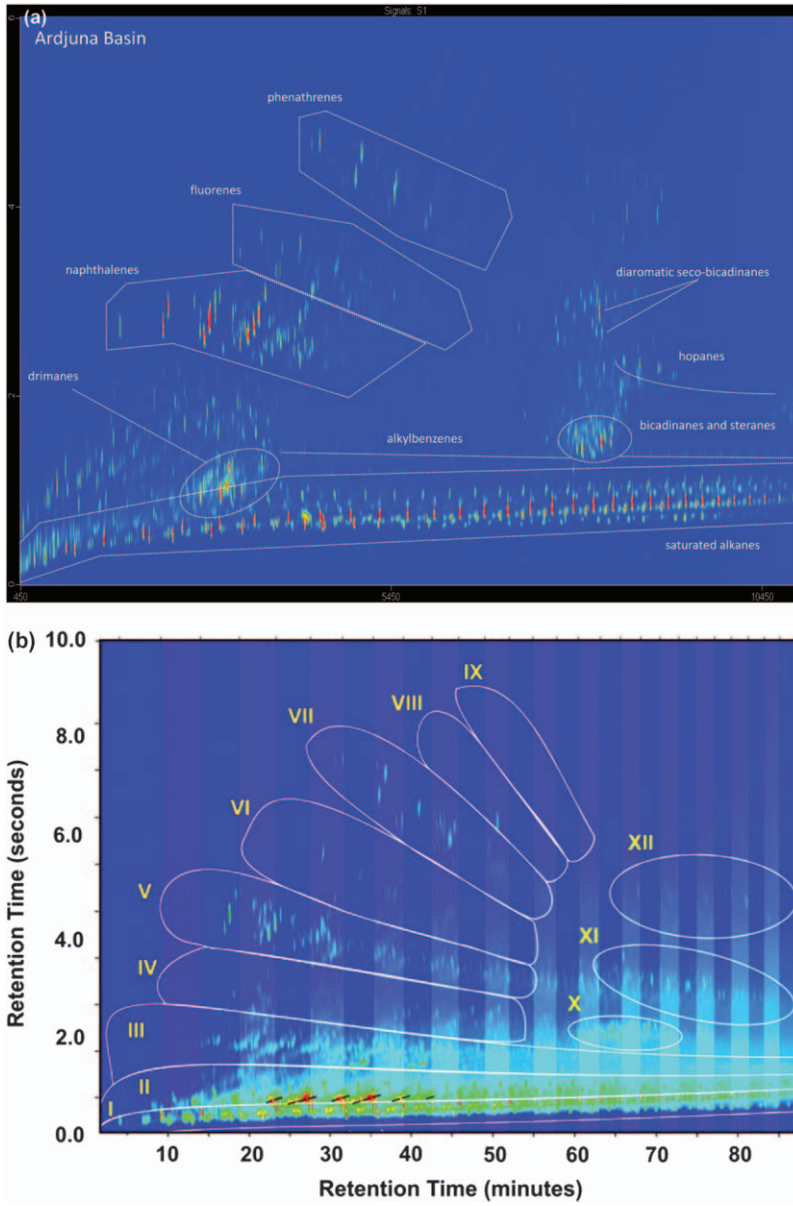

Figure 12.3 GC×GC-FID contour plots highlighting the compound class elution order and pattern with a non-polar/polar column configuration. a) Oil from the Ardjuna Basin (Indonesia), b) Oil P-2 described by Ventura *et al.*[24] I, normal and branched alkanes; II, cycloalkanes; III, alkyl benzenes and tricyclic terpanes; IV, indenes; V, naphthalenes and benzothiophenes; VI, fluorenes; VII, phenanthrenes and dibenzothiophenes; VIII, fluoranthenes; IX, pyrenes; X, steranes; XI, hopanes, and XII, benzohopanes.
Reprinted from Ventura *et al.*,[24] Copyright (2010), with permission from Elsevier.

along the increasing second dimension retention time in the general order of tricyclic triterpenoids < tetracyclic triterpenoids < pentacyclic triterpenoids (Figure 12.3).

Aromatic compounds (all rings aromatic) elute only slightly later in the first dimension while the second-dimension retention time increases rapidly with each additional aromatic ring in the order (groups including all alkyl derivatives): benzenes < alkylbenzenes (overlapping with tricyclic terpenanes < indenes < naphthalenes and benzothiophenes < fluorenes < phenanthrenes and dibenzothiophenes < fluoranthenes < pyrenes (Figure 12.3).[24]

Similarly, series of compounds such as pentacyclic triterpenoids demonstrate rapidly increasing second-dimension RT with progressing aromatisation, facilitating the study of diagenetic degradation products in a geological sample.

Biomarker classes such as hopanoids or steroids elute as groups within the chromatographic plane. Within one biomarker group, a slight difference in first- and/or second-dimension retention time can be related to changes in the structure relative to the base structure. Reliable identification of biomarkers is achieved based on the first- and second-dimension RT and the biomarker fingerprint within the distinct elution pattern of the compound classes. For example, naturally occurring 17β,21β(H)-hopanes and the series of altered epimers, such as C_{27}–C_{35} 17β,21α(H)-moretanes, 17α,21β(H)-hopanes, 25-norhopanes are separated by GC×GC not only in the first dimension, as in traditional 1D GC, but also in the second dimension (Figure 12.4), resolving coelution of hopanes with very similar mass spectra.[18] 25-Norhopanes elute relatively early in the second dimension, well before regular α,β-hopanes followed by the β,α-hopanes (moretanes). The longest RT were observed for the β,β-hopanes, which elute considerably later in the second dimension. All series create a distinct, recognisable pattern in the chromatogram (Figure 12.4).

All common steranes are well separated in the first and second dimension (Figure 12.4). Diasteranes elute earlier in the second dimension of a non-polar/polar column configuration and are well separated from the regular steranes. Furthermore, in traditional 1D chromatograms steranes and bicadinanes coelute with the separation being even more complicated because the characteristic mass fragment ion for steranes (*m/z* 217) is also present in bicadinanes. As a consequence, GC-MRM-MS analysis is often required for reliable quantification of these two biomarker groups. In GC×GC-TOF-MS chromatograms, both compound classes elute well separated in the second dimension (Figure 12.4).[27]

GC×GC analysis of whole oils facilitates identification of diagenetically related products. Saturated, mono-, di-, and triaromatic tetracyclic triterpenoids can easily be determined with the help of the two RT. Increasing secondary retention time responds to increasing polarity, *i.e.* aromaticity; mono-, di-, and triaromatic compounds elute along a line within the 2D chromatogram plane.

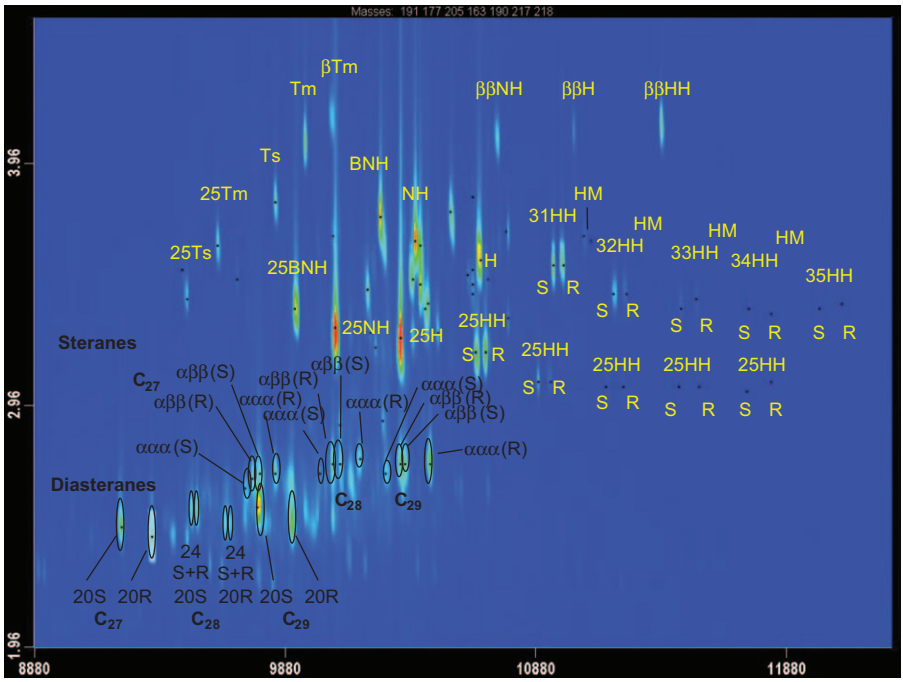

Figure 12.4 Separation of hopanes (yellow) and steranes (black) using GC×GC-TOF. Shown is the combined EIC of the masses *m/z* 191, 177, 205, 163, 190, 217, and 218. H, hopane; 25, 25-norhopane; HH, homohopane; HM, homomoretane; NH, norhopane; BNH, bisnorhopane.
Reprinted from Eiserbeck *et al.*,[27] Copyright (2012), with permission from Elsevier.

12.3 Superiority of GC×GC Compared to Traditional 1D Techniques?

12.3.1 Comparison to GC-MS and GC-MRM-MS

The superiority of GC×GC over more traditional 1D gas chromatographic techniques is evident in every GC×GC application presented in the literature. Eiserbeck *et al.*[27,67] demonstrated the separation and resolution improvement of GC×GC in comparison with traditional 1D GC as well as metastable reaction monitoring techniques like GC-MRM-MS.

Most important to note is the improved resolution down to minor detailed biomarker regions with only one analysis of the whole fluid. A similarly detailed result using GC-MS or GC-MRM-MS required one to multiple separation steps prior to the analysis such as liquid chromatography, molecular sieving, argentation chromatography, *etc.*, all of which can cause losses, carry the risk of contamination of the sample, and are time consuming. Subsequently, a series of different GC and MS methods (GC-MS and GC-MRM-MS) have to be applied which are customised to the relevant fraction

or compound class in order to achieve the resolution and detail required. These methods can include scans, SIM, and multiple reaction monitoring (MRM) tailored to different questions and applied to multiple fractions of the sample (saturates, branched/cyclics, unsaturated hydrocarbons, aromatics and possibly the polars such as porphyrins. To achieve the full detailed picture of the composition of one sample can easily require up to 10 or even 20 individual analyses.

GC×GC separation can accomplish this detail in one single analysis without losing the detail of the mass spectra. GC-MRM-MS for example achieves high sensitivity and can separate coeluting compounds by limiting the acquisition to very specific parent-daughter-ion transitions. However, the resulting chromatograms lack the information of the full mass spectrum and identification of the peaks is limited to one or a handful of transitions and the retention time. An example of the spatial resolution achieved by GC×GC compared to coelution in GC-MS and separation resulting from monitoring of limited transitions as applied in GC-MRM is the coelution of bicadinanes with steranes as mentioned in section 12.2.6.

Furthermore, analysis of fractions using specified mass spectrometry methods masks the whole picture of a sample because each one of these analyses is only representing a small portion of the whole sample.

GC×GC-TOF-MS is the only gas chromatographic system that can acquire molecular data of the whole sample in high detail. A direct comparison of the relative abundances of saturated and aromatic compounds can be achieved, allowing for instant fingerprinting (see section 12.4.1) of oils, condensates and rock extracts.

12.3.1.1 Biodegradation

Gas chromatographic analysis of severely biodegraded samples with the traditional 1D technique often presents a challenge due to the extensive 'hump' of unresolved complex mixture (UCM). With GC-MS analysis, the chromatogram of the saturated hydrocarbon fraction of a severely biodegraded oil is dominated by UCM with only information retained of the remaining compounds. Mass spectra of the remaining compounds are often unclear due to low concentrations and can lead to loss of information of the molecular ion. Injection of higher concentrated sample could resolve this problem however the general resolution of the sample is disturbed by the increasing amount of UCM. Furthermore, injection of more UCM to the capillary column can cause damage to the column and significantly reduce its lifetime.

While the resolution and quantification of a limited number of compounds can be improved by applying a SIM, Figure 12.5a), the UCM still adds significant noise to the mass spectra and alters the baseline of the SIM chromatogram.

Application of GC-MRM-MS reduces the rise in the baseline caused by the UCM to near zero (Figure 12.5b) and increases the sensitivity for a few selected compounds (depending on the transitions chosen for a particular

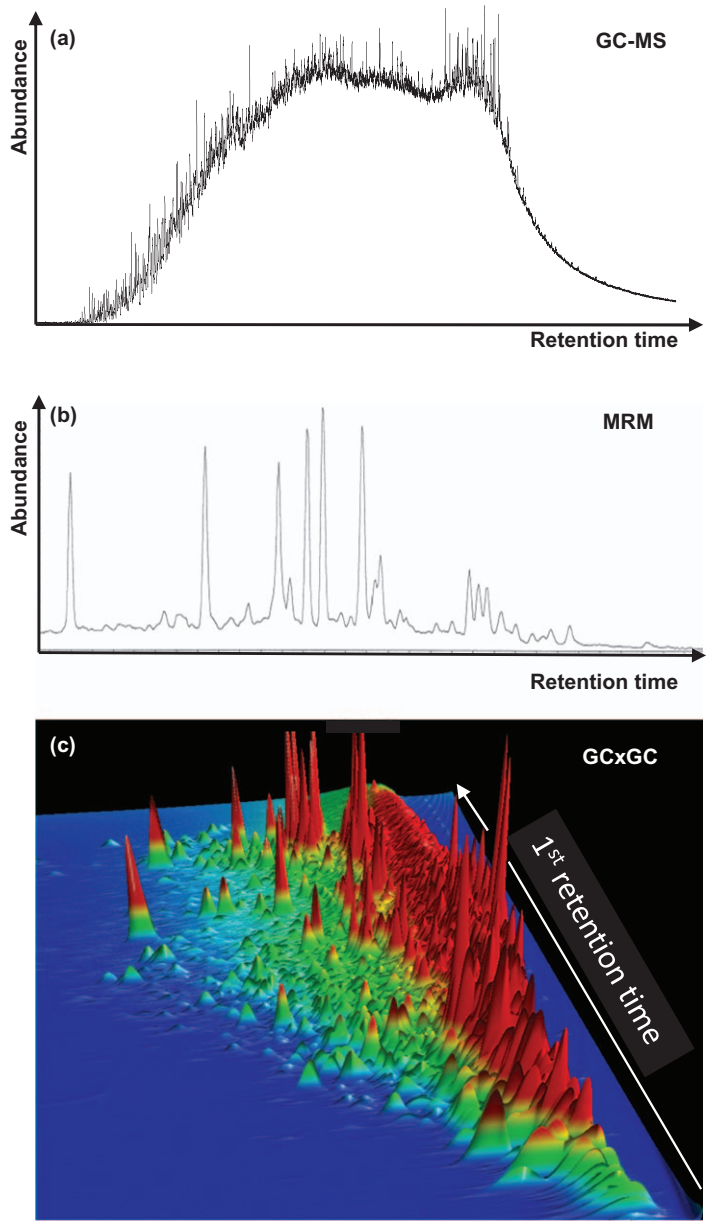

Figure 12.5 Comparison of the resolution of unresolved complex mixture (UCM) using (a) GC-MS, (b) GC-MRM-MS, and (c) Mountain plot of a GC×GC-FID analysis.
Reprinted from Eiserbeck *et al.*,[27] Copyright (2012), with permission from Elsevier.

method). However, screening of a biodegraded sample and retaining all mass spectral information needed for identification is not possible. GC-MRM-MS relies on only a few transitions per compound for

identification, which increases the sensitivity but prevents positive identification of many biomarkers based on their mass spectra.

The second-dimension separation in GC×GC-TOF-MS resolves most of the compounds from the UCM in a whole-oil sample without significant losses in sensitivity and retains full mass spectral information for identification (see also section 12.4.3). Figure 12.5c illustrates the improvement in separation of a severely biodegraded oil.

12.3.1.2 Thermal Maturity

Assessment of thermal maturity of a geological sample using established biomarker ratios[68] is an important part of the screening and interpretation of a sample. Silva *et al.*[20] demonstrated the use of thermal maturity parameters from GC×GC-TOF-MS. But how do these parameters compare to data obtained from 1D GC techniques? Are they comparable to the extensive and valuable database of maturity parameters obtained in the past decades? Eiserbeck *et al.*[27] evaluated this question by comparing results for the isomerisation ratio $S/(S+R)$ of C_{32} homohopanes, one of the most commonly applied thermal maturity parameters,[68] obtained from GC-MS, GC-MRM-MS, GC×GC-FID, and GC×GC-TOF-MS. GC×GC data proved to be comparable with the more traditional techniques (Figure 12.6). The $22S/(22S+22R)$ ratios obtained from all four techniques were in very good agreement for the analysed samples in this study, generally within analytical error (≤5%). A few outliers were observed for severely biodegraded samples in which maturity

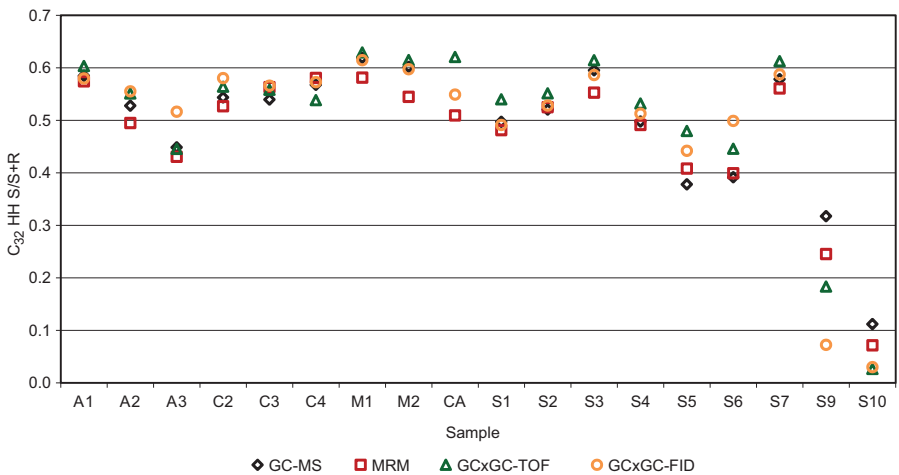

Figure 12.6 Comparison of thermal maturity parameters calculated from data derived from GC-MS, GC-MRM-MS, GC×GC-FID and GC×GC-TOF. The C_{32} homohopane ratio C_{32} S/(S + R) was chosen as a representative parameter for thermal maturity.
Reprinted from Eiserbeck *et al.*,[27] Copyright (2012), with permission from Elsevier.

parameters based on biomarker concentration are unreliable and alternative methods for the assessment of thermal maturity are recommended.

This result carries importance for the application of GC×GC for oil and rock screening, acquisition of much better resolved molecular data, and comparability to biomarker data reported in the past based on 1D analysis.

12.4 Applications of GC×GC in Geochemical Studies

The application of GC×GC in the geosciences is has increased significantly over the last 5–10 years. Summaries of less recent geochemical studies using GC×GC can be found in the reviews by Adahchour *et al.*[5,6,14]

This section focuses on recent applications and introduces concepts developed for tackling long-known separation problems such as the resolution of UCMs using GC×GC as well as approaches for the processing of the enormous amounts of data derived from GC×GC analyses.

12.4.1 Fingerprinting

GC×GC chromatograms of whole oils or sediment extracts provide an easy way for the first assessment of a fluid including dominant compound classes beyond the n-alkanes, which are mostly all that can be observed in a total ion chromatogram of traditional 1D GC. Geological samples can be compared in much more detail with just a quick glance at the 3D chromatogram (Figure 12.7).

Aromatic compounds elute further in the polar dimension than saturated compounds, and thus can be distinguished easily in whole-oil analysis. Most abundant compounds, compound classes, main features, and general similarities or differences between oils (Figure 12.7) appear clearly in much more detail than is possible using traditional 1D GC analysis.

Li *et al.*[26] used GC×GC in combination with sulfur isotope analysis to fingerprint petroleum fluids that are affected by thermochemical sulfur reduction (TSR). The authors clearly identified indicators for TSR in fluids from the Canadian Upper Devonian Nisku Formation and the Chinese north-eastern Jinxian Sag of Bohai Bay Basin. Molecular indicators of TSR in 'sour' condensates included lower saturated to aromatic hydrocarbon ratios ($\sim$2; for comparison 'sweet' oils commonly have a ratio of $\sim$ 5), a high molar concentration of hydrogen sulfide in the associated gas ($\sim$20% *vs.* $<$1% in sweet oils) and most importantly a strong predominance of sulfur-containing heterocyclics such as benzothiophenes and dibenzothiophenes over the common polycyclic aromatic hydrocarbons and diagenetically derived sulfur-bound biomarkers, clearly separated and identified in the GC×GC chromatogram (Figure 12.8).[26]

As described in section 12.2.6, chemical compound classes elute in a GC×GC chromatogram in clusters that can be grouped and also quantified as a group.

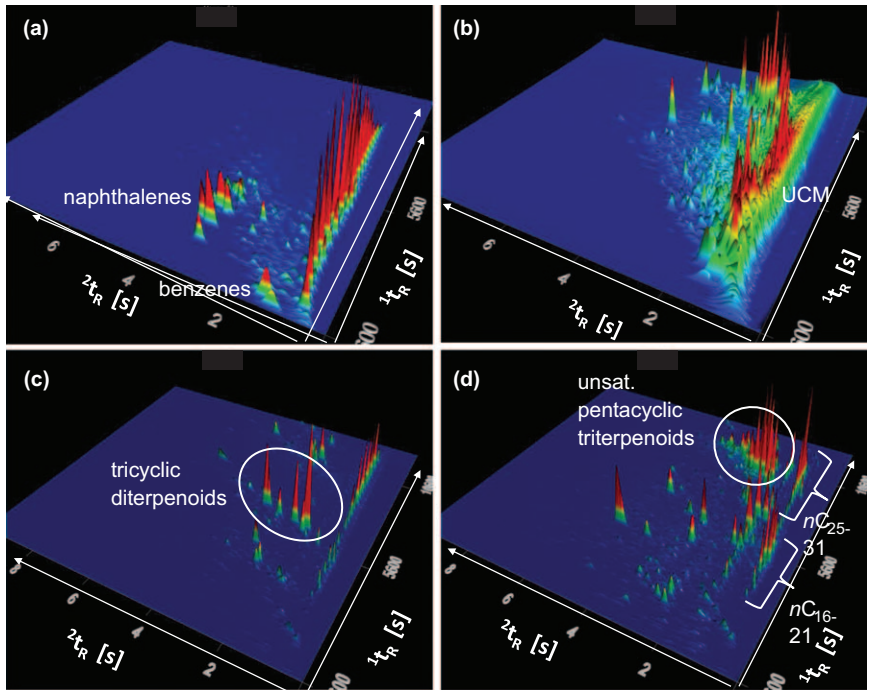

Figure 12.7 3D Mountain plots of GC×GC-FID chromatograms for two crude oils (a and b), and two sediment extracts (c and d). Highlighted compound classes group together and clearly indicate the main features of a sample in a spatial context. ^1t_R and ^2t_R are primary and secondary retention time, respectively and are given in seconds. Abundances are colour coded (blue = baseline, colour change from green to red with increasing abundance) and relative to the most abundant peak in each chromatogram. Reprinted from Eiserbeck *et al.*,[27] Copyright (2012), with permission from Elsevier.

The combination of high-resolution separation and quality quantification possibilities, and the grouping of compound classes can be applied to fingerprint fluids and compare them with regard to thermal maturity, source, degree of biodegradation, *etc.* Applying the full range of GC×GC capabilities, Ventura *et al.*[24] presented a method to identify compositional differences or similarities in oils, which is a defining question in oil reservoir characterisation. The method included a comparison of biomarkers that reflect thermal maturity and source of organic matter, a group comparison of compound classes, and comparison of compound classes across a specified retention index range. Quantitative assessment of oil similarities over a range of carbon numbers using traditional 1D GC techniques required a series of calibration standards and curves and was still limited to n-alkanes, iso-, cycloalkanes, and aromatic compounds.[69,70] With GC×GC the range of

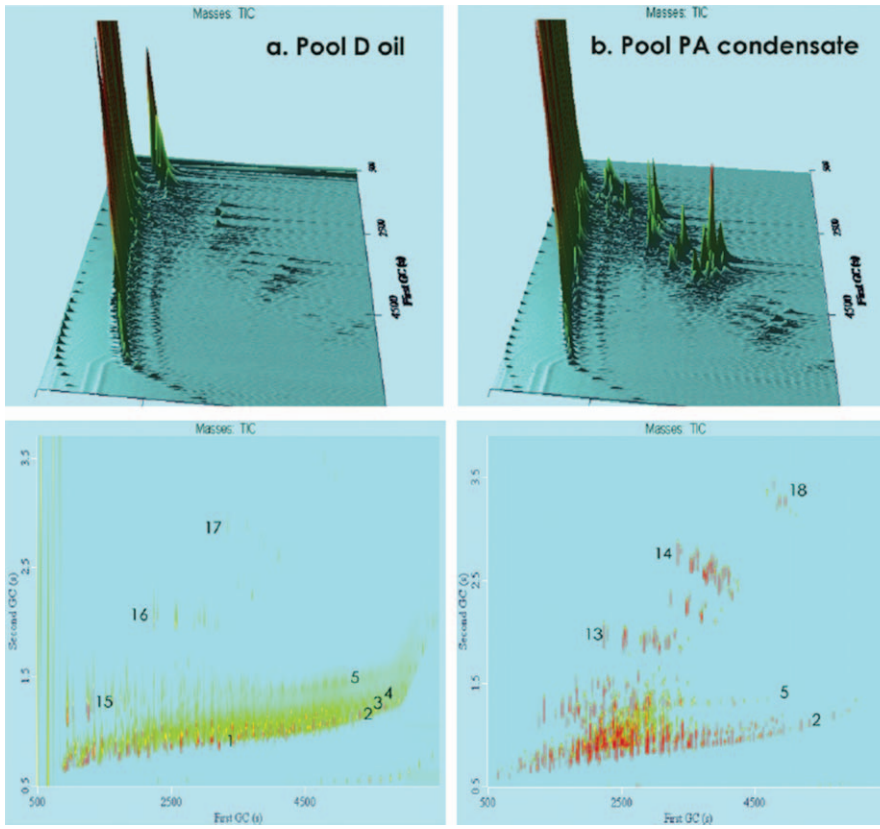

Figure 12.8 GC×GC chromatograms of fluids from the Brazeau River field, west-central Alberta (Canada). (a) Pool D oil, a 'sweet' oil without molecular signs of TSR. (b) Pool PA condensate with high abundance of benzothiophenes and dibenzithiophenes indicating TSR. (1) isoprenoid alkanes; (2) n-alkanes; (3, 4) alkylcyclopentanes and alkylcyclohexanes; (5) alkylbenzenes and alkyltoluenes including aryl isoprenoid alkanes; (6) steranes and methyl steranes; (7) pentacyclic terpanes; (8) hexahydrobenzohopanes; (9) thiolane and thiophene steroids; (10) thiolane and thiophene hopanoids; (11) monoaromatic steroids; (12) triaromatic steroids; (13) alkyl benzothiophenes; (14) alkyl dibenzothiophenes; (15) alkyl benzofurans; (16) alkyl naphthalenes; (17) alkyl phenanthrenes; (18) alkyl-9-thia-1,2-benzofluorenes.
Reprinted from Li *et al.*,[26] Copyright (2012), with permission from Elsevier.

comparable compound classes was extended to *e.g.* hopanes, steranes, mono- and dicyclic alkanes, naphthalenes and benzothiophenes, indenes, fluorenes, pyrenes, triaromatic steranes and benzohopanes, and more. Additionally, the resolving and data mining power of GC×GC could be utilised to identify minor chemical differences to a level that is not achievable with 1D GC.

These oil fingerprinting techniques are highly applicable to study oil reservoir compartmentalisation, migration effects, reservoirs with current charges that have not reached equilibrium, and other transformation processes.

12.4.1.1 *Monitoring of Degradation Processes—Oil Spill Modelling*

Oil is introduced to the environment naturally through oil seeps but also through incidents during exploration activities caused by human or technical failure. Oil spills have occurred regularly throughout the decades of oil exploration and transport. The fate of the expelled oil lies in biological degradation, evaporation, and water-washing. However, the exact processes and degree to which each of these processes contribute has not been very well understood in the past.

Furthermore, the question of identifying the exact source of spilled oil[52] is crucial to identifying the causes of the spill and prevention of similar incidents in the future, and also for legal matters. Understanding the exact degradation processes is important for development of effective spill clean-up. GC×GC has proven to be a very useful tool to track the weathering process and shed some light on the source and true fate of spilled hydrocarbons.

Nelson *et al.*[48] studied the weathering progress of the No. 6 fuel oil that was released into Buzzards Bay (Massachusetts, USA) in 2003 when the single-hulled barge *Bouchard 120* grounded. Samples were collected from oil covered rocks on days 12 and 179 after the accident. The GC×GC chromatograms of these two samples clearly showed the weathering (biodegradation, water-washing, and evaporation) and most affected compound classes could be identified as n-alkanes, alkylated naphthalenes, and phenanthrenes. A more sophisticated way to determine the changes between day 12 and day 179 was presented in form of difference, ratio, and addition chromatograms (Figure 12.9).

The difference chromatogram was obtained by normalising both chromatograms to 17α(H),21β(H)-hopane followed by the subtraction of the day 179 chromatogram from the day 12 chromatogram. Retention time stability was validated prior to this step. The resulting difference chromatograms (Figure 12.9 and Figure 12.10.a) show clearly all the compounds and compound classes that were reduced or eliminated between the two sampling events.

The ratio plot (Figure 12.10b) is a difference chromatogram resulting from the division of the slightly weathered sample (day 12) by the heavily weathered sample (day 179). Red peaks exhibit the largest relative loss from weathering. The addition chromatogram (Figure 12.10c) indicates compounds that are either completely removed from the slightly weathered sample (green) or were not present in the spilled oil sample at day 12 but

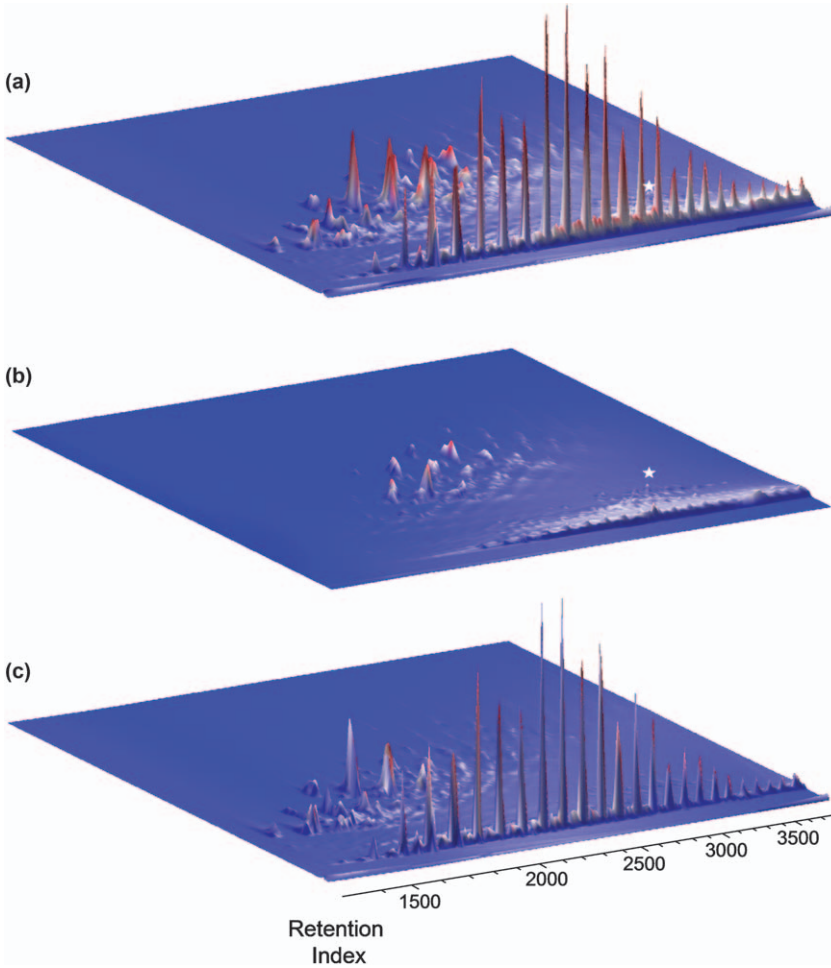

Figure 12.9 GC×GC mountain plot chromatogram of sample extracts from Bouchard 120 oil-covered rocks collected (a) 12 days after the spill (9 May 2003), and (b) 179 days after the spill (23 November 2003). The conserved standard 17α(H)-21β(H)-hopane is marked with a star. Reprinted from Nelson *et al.*,[48] Copyright (2006), with permission of the publisher Taylor & Francis Ltd (http://www.tandf.co.uk/journals).

were present on day 179 (red), representing compounds that have been formed during the degradation process. The results showed a transition from n-alkanes to polyaromatic hydrocarbon (PAH)-dominated hydrocarbons over the course of 6 months. During that time, 20–100% of the n-alkanes were removed, while hopanes and steranes changed very little. Image-based techniques like difference chromatograms identified weathering trends and facilitate source identification and monitoring of natural and enhanced bioremediation of petroleum hydrocarbons.

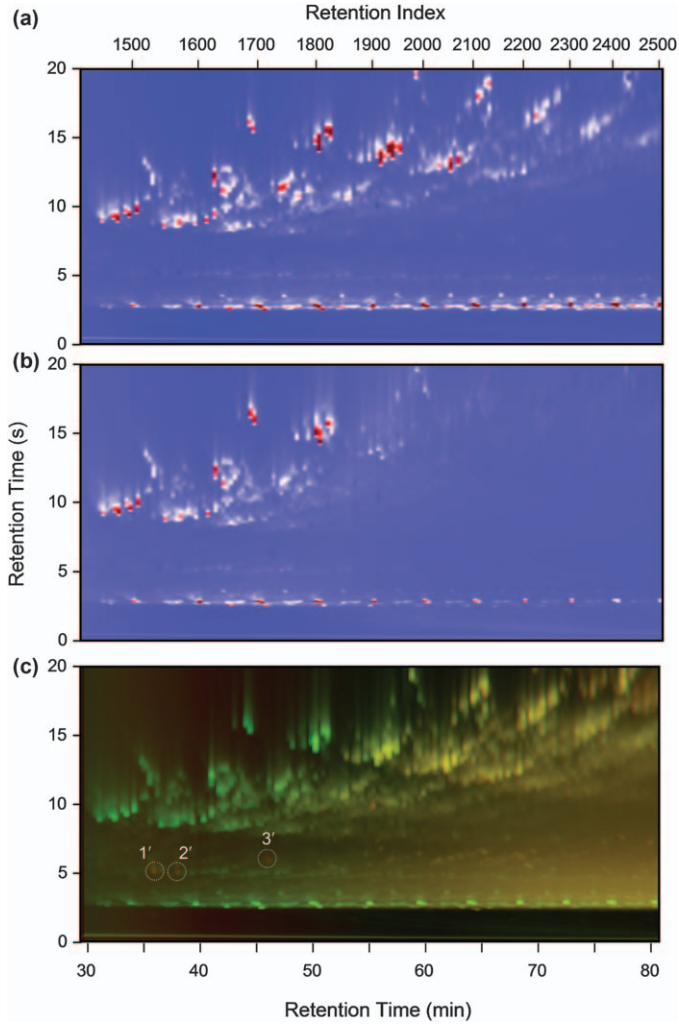

Figure 12.10 Enlarged GC×GC colour contour (a) difference chromatogram, (b) ratio chromatogram, and (c) addition chromatogram. Peak intensities in (a) and (b) are colour coded from white to red (most abundant). The addition chromatogram was produced using both colour and intensity values for each chromatogram. All the peaks in the day 12 (9 May 2003) chromatogram were assigned the colour green, and all the peaks from the day 179 (23 November 2003) chromatogram were assigned the colour red. Compounds that are present in one chromatogram but are absent in the other appear either green or red; compounds that are present in both chromatograms appear yellow. Red peaks at the left of the chromatogram (labelled 1, 2, and 3; c) indicate either that these compounds were not present in any appreciable amount in the day 12 chromatogram or that these compounds are preferentially conserved while proximal compounds are lost during oil weathering.
Reprinted from Nelson *et al.*,[48] Copyright (2006), with permission of the publisher Taylor & Francis Ltd (http://www.tandf.co.uk/journals).

Peacock *et al.*[49] characterised the residual petroleum hydrocarbons in salt marsh sediments in Winsor Cove (Buzzards Bay, Massachusetts), impacted from the 1974 spill of No. 2 fuel oil by the barge *Bouchard 65*. Significant amounts of PAHs, mainly C_4-naphthalenes and C_1-, C_2-, and C_3-phenenthrenes/anthracenes remained in the upper sediment layers whereas naphthalene and phenanthrene were removed. Biodegradation, evaporation, and water-washing as well as erosion were identified as removal processes.

Lemkau *et al.*[47] studied the weathering of heavy fuel oils from the MV *Cosco Busan* spill (November 2007; San Francisco Bay, CA, USA). They related the spilled oil to the exact source (ruptured tank 3 or 4) and characterised changes in the oil composition across location and time. Changes in n-C_{18}/phytane and benz[*a*]anthracene/chrysene ratios indicated biodegradation and photodegradation as causes of compound removal or decrease.

GC×GC has been applied extensively for studies of the fate of the oil after the Deepwater Horizon disaster.[42,50,71–74] On 20 April 2010 an explosion and fire aboard the drilling rig *Deepwater Horizon* in the Gulf of Mexico killed 11 crew members and marked the beginning of the largest offshore oil spill ever to occur in US territorial waters. The *Deepwater Horizon* capsized and sank on 21 April 2010, coming to rest approximately 400 m north-west of the well head at a depth of approximately 1500 m. Crude oil from the Macondo well flowed into the northern Gulf of Mexico between 20 April and 4 August 2010 (approximately 106 days) before the well was finally sealed with drilling mud and cement. Over the course of the spill an estimated 4.9 million barrels of oil flowed into the Gulf of Mexico, according to a US Federal On Scene Coordinators (FOSC) report.[75] Oil from the spill was found on beaches and in marshes in Texas, Louisiana, Mississippi, Alabama, and Florida.

Fingerprinting weathered oil and tar balls from this spill is challenging because (1) the crude oil was transported vertically through the water column from a depth of 1500 m to the surface; (2) the sea-surface water temperature was 30 °C and higher; (3) chemical dispersants were used both at the sea surface (initially) and at the well head; (4) *in situ* burning of oil at the sea surface took place; and (5) solar radiation is capable of transforming some of the chemical components in crude oil. The combined weathering processes of water-washing, evaporation, photooxidation, and biodegradation altered the composition of spilled oil dramatically in many instances.

It became apparent shortly after the spill began that the most useful region of the 2D gas chromatogram for fingerprinting weathered oil samples in order to determine the source of spilled oil found on beaches of the northern Gulf of Mexico was the biomarker region and the hopanoids in particular appeared to be environmentally recalcitrant and thus very good molecules for fingerprinting (Figure 12.11a).[76] The advantage of using GC×GC for fingerprinting oil found on beaches and floating at the sea

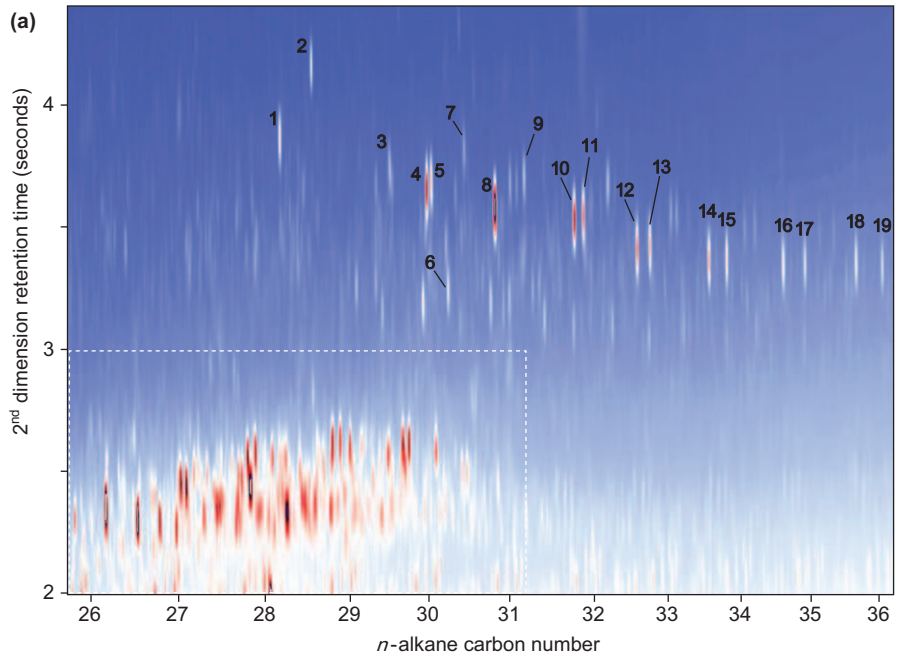

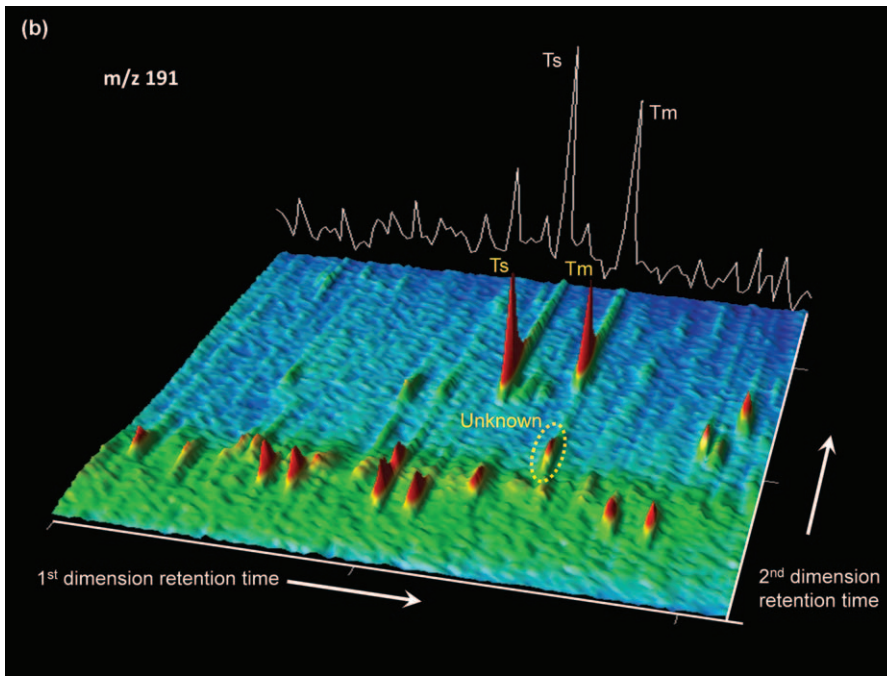

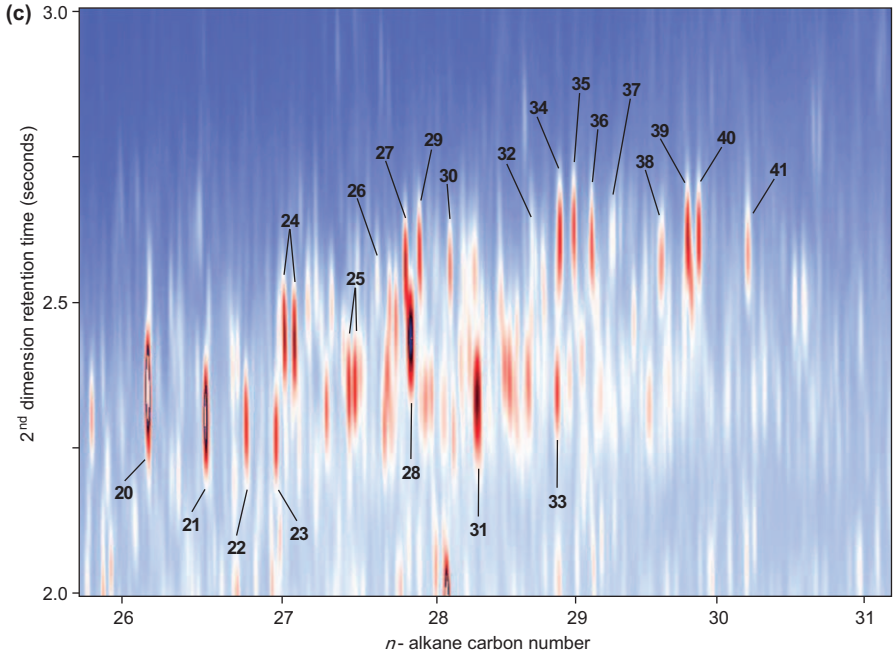

Figure 12.11 (a) Colour contour plot of the biomarker region of Macondo well crude oil. In this figure the hopanoid components are numbered and the chemical names, molecular formulas, and masses are shown in Table 12.2. The area highlighted inside the yellow box (diasteranes and steranes) is expanded in Figure 12.11c. (b) Example of a coelution that is readily apparent using GC×GC but frequently overlooked by laboratories using standard GC-MS. When laboratories integrate the unknown and the Tm peak together as one peak the Ts/Tm ratio underestimates the thermal maturity of the crude oil being studied. (c) This figure highlights the complexity of the sterane/diasterane region of Macondo well crude oil.

surface is the very high resolving power of the GC×GC technique compared to standard GC techniques. 2D GC affords approximately 10× more resolution compared with traditional GC. There are numerous examples of biomarker components that coelute in 1D GC which are resolved using GC×GC.

Figure 12.11b highlights the coelution of an unknown component and 17α-22,29,30-trisnorhopane (Tm). The unknown component eluting with Tm on GC-MS instruments produces an *m/z* 191 ion and this component elutes directly below the Tm molecule in 2D chromatographic space. Laboratories that utilise the Ts/Tm thermal maturity indicator ratio (Ts: 18α-22,29,30-trisnorhopane) using standard GC-MS techniques underestimate the thermal maturity of crude oils when this unknown component is present and integrated together with the Tm peak (as in the case of Macondo oil).

Table 12.2 Key to the compounds labelled in Figure 12.11.

Peak no.	Abbreviation	Compound name and formula	Mass
1	Ts	18α(H)-22,29,30-trinorneohopane ($C_{27}H_{46}$)	370
2	Tm	17α(H)-22,29,30-trinorhopane ($C_{27}H_{46}$)	370
3	BNH	17α(H),21β(H)-28,30-bisnorhopane ($C_{28}H_{48}$)	384
4	NH	17α(H),21β(H)-30-norhopane ($C_{29}H_{50}$)	398
5	C29-Ts	18α(H),21β(H)-30-norneohopane ($C_{29}H_{50}$)	398
6	C30-Dia	17α(H),21β(H)-diahopane ($C_{30}H_{52}$)	412
7	NM	17β(H),21α(H)-30-norhopane ($C_{29}H_{50}$) normoretane	398
8	H	17α(H),21β(H)-hopane ($C_{30}H_{52}$)	412
9	M	17β(H),21α(H)-hopane ($C_{30}H_{52}$) moretane	412
10	HH (S)	17α(H),21β(H)-22S-homohopane ($C_{31}H_{54}$)	426
11	HH (R)	17α(H),21β(H)-22R-homohopane ($C_{31}H_{54}$)	426
12	2HH (S)	17α(H),21β(H)-22S-bishomohopane ($C_{32}H_{56}$)	440
13	2HH (R)	17α(H),21β(H)-22R-bishomohopane ($C_{32}H_{56}$)	440
14	3HH (S)	17α(H),21β(H)-22S-trishomohopane ($C_{33}H_{58}$)	454
15	3HH (R)	17α(H),21β(H)-22R-trishomohopane ($C_{33}H_{58}$)	454
16	4HH (S)	17α(H),21β(H)-22S-tetrakishomohopane ($C_{34}H_{60}$)	468
17	4HH (R)	17α(H),21β(H)-22R-tetrakishomohopane ($C_{34}H_{60}$)	468
18	5HH (S)	17α(H),21β(H)-22S-pentakishomohopane ($C_{35}H_{62}$)	482
19	5HH (R)	17α(H),21β(H)-22R-pentakishomohopane ($C_{35}H_{62}$)	482
20	DiaC_{27}βα-20S	13β(H),17α(H)-20S-diacholestane ($C_{27}H_{48}$)	372
21	DiaC_{27}βα-20R	13β(H),17α(H)-20R-diacholestane ($C_{27}H_{48}$)	372
22	DiaC_{27}αβ-20S	13α(H),17β(H)-20S-diacholestane ($C_{27}H_{48}$)	372
23	DiaC_{27}αβ-20R	13α(H),17β(H)-20R-diacholestane ($C_{27}H_{48}$)	372
24	DiaC_{28}βα-20S	24-methyl(S&R)-13β(H),17α(H)-20S-diacholestane ($C_{28}H_{50}$)	386
25	DiaC_{28}βα-20R	24-methyl(S&R)-13β(H),17α(H)-20R-diacholestane ($C_{28}H_{50}$)	386
26	C_{27}ααα-20S	5α(H),14α(H),17α(H)-20S-cholestane ($C_{27}H_{48}$)	372
27	C_{27}αββ-20R	5α(H),14β(H),17β(H)-20R-cholestane ($C_{27}H_{48}$)	372
28	DiaC_{29}βα-20S	24-ethyl(S&R)-13β(H),17α(H)-20S-diacholestane ($C_{29}H_{52}$)	400
29	C_{27}αββ-20S	5α(H),14β(H),17β(H)-20S-cholestane ($C_{27}H_{48}$)	372
30	C_{27}ααα-20R	5α(H),14α(H),17α(H)-20R-cholestane ($C_{27}H_{48}$)	372
31	DiaC_{29}βα-20R	24-ethyl(S&R)-13β(H),17α(H)-20R-diacholestane ($C_{29}H_{52}$)	400
32	C_{28}ααα-20S	24-methyl-5α(H),14α(H),17α(H)-20S-cholestane ($C_{28}H_{50}$)	386
33	DiaC_{29}αβ-20R	24-ethyl(S&R)-13α(H),17β(H)-20R-diacholestane ($C_{29}H_{52}$)	400
34	C_{28}αββ-20R	24-methyl-5α(H),14β(H),17β(H)-20R-cholestane ($C_{28}H_{50}$)	386
35	C_{28}αββ-20S	24-methyl-5α(H),14β(H),17β(H)-20S-cholestane ($C_{28}H_{50}$)	386
36	Unknown	Unknown ($C_{29}H_{52}$)	400
37	C_{28}ααα-20R	24-methyl-5α(H),14α(H),17α(H)-20R-cholestane ($C_{28}H_{50}$)	386
38	C_{29}ααα-20S	24-ethyl-5α(H),14α(H),17α(H)-20S-cholestane ($C_{29}H_{52}$)	400
39	C_{29}αββ-20R	24-ethyl-5α(H),14β(H),17β(H)-20R-cholestane ($C_{29}H_{52}$)	400
40	C_{29}αββ-20S	24-ethyl-5α(H),14β(H),17β(H)-20S-cholestane ($C_{29}H_{52}$)	400
41	C_{29}ααα-20R	24-ethyl-5α(H),14α(H),17α(H)-20R-cholestane ($C_{29}H_{52}$)	400

An expanded view of the region of the GC×GC chromatogram that contains diasteranes and steranes is presented in Figure 12.11c (this is the area highlighted by a yellow box in Figure 12.11a). This figure illustrates the complexity of the diasterane/sterane region as well as the resolving power of the GC×GC technique. This level of resolution is unattainable by conventional GC techniques, and coeluting peaks (that are frequently misinterpreted) are resolved from one another here. Examples of components that coelute on standard GC instruments but are resolved using GC×GC are seen as peaks 27 and 28 and peaks 33 and 34 in Figure 12.11c. Peaks 27 and 28 are 5α(H),14β(H),17β(H)-20*R*-cholestane and 24-ethyl(*S*&*R*)-13β(H),17α(H)-20S-diacholestane respectively and commonly coelute on 1D instruments. Using GC×GC, these two coeluting components are very nearly completely resolved. Likewise, peaks 33 and 34, (24-ethyl(*S*&*R*)-13α(H),17β(H)-20*R*-diacholestane and 24-methyl-5α(H),14β(H),17β(H)-20*R*-cholestane), coelute on 1D instruments but are completely resolved using GC×GC. Close inspection of this chromatogram highlights many more components that coelute on 1D instruments that are resolved on GC×GC instruments (see the small coeluting peak to the lower right of peak 39, for example).

The detailed characterisation by GC×GC of the Macondo oil and gas end member sampled directly from the well head was applied by Reddy *et al.*[50] to determine the gas-to-oil ratio (GOR), as well as the trajectories and fates of the hydrocarbons in the deep water marine environment. In contrast to oil spills at the sea surface, where evaporation and dissolution are equally important factors in the removal of hydrocarbons, deep water spills such as the *Deepwater Horizon* disaster at 1.5 km depth lack the evaporative component in the fate of the hydrocarbons. Compositional comparison of the released Macondo fluid and samples taken from the water column within a deep water plume that was defined by Camilli *et al.*[77] make it possible to study the partitioning of hydrocarbons into the aqueous phase in the absence of atmospheric evaporation.

Detailed compositional analysis of the whole fluid showed that the total C_1–C_5 hydrocarbon fraction accounted for half of the mass of hydrocarbons released from the Macondo well. These light hydrocarbons are commonly not detected by traditional oil characterisation methods on a molecular level, which can lead to significant underestimation of the total hydrocarbon mass released during a spill.

Compositional analyses of the hydrocarbon content in the deep water plume at 1100 m depth indicated that the hydrocarbon levels of low-molecular-weight n-alkanes and aromatic compounds were below their saturation levels. Furthermore, evidence was found that methane was quantitatively trapped in the deep water plume and was nearly absent in shallower depths of the water column. With increasing chain length (C_2, C_3, *etc.*), less n-alkanes were dissolved in the deep water plume due to their decreasing solubility in water. With increasing molecular mass an increasing proportion of the total n-alkane content was retained in the buoyant liquid oil phase ascending to the sea surface. Water-soluble aromatic compounds

were also monitored in their coexistence to n-alkanes and their decrease in abundance over 27 km of trajectory of the plume. Data by Reddy *et al.*[50] indicate no significant biodegradation progress in aromatic compounds over 27 km (4 days).

Overall, it was demonstrated that most of the C_1–C_3 hydrocarbons and water-soluble aromatic compounds were retained in the deep water column while less soluble components were transported to the surface or sank to the sea floor.

Natural seeps contribute almost half of the oil entering the coastal ocean. Nonetheless, the rates and relevance of physical, chemical, and biological weathering processes are poorly understood. Wardlaw *et al.*[51] studied natural oil seeps offshore Santa Barbara, California, USA with comprehensive 2D GC to investigate the specific changes in petroleum composition and hydrocarbon abundance between subsurface reservoirs, a proximal sea floor seep, and the sea surface overlying the seep. The group developed methods to account for hydrocarbon mass losses to the different processes including biodegradation, dissolution, and evaporation differentiating biological and physical weathering processes of complex mixtures at a molecular level using GC×GC.

Similarly, Farwell *et al.* studied the long-term fate and fallout plume of heavy oil from strong natural petroleum seeps near Coal Oil Point, California.[46]

12.4.1.2 Statistical Analysis of GC×GC Data

Ventura *et al.*[22] extended their fingerprinting approach and applied statistical methods to effectively data-mine the large molecular data sets obtained by a high-resolution technique such as GC×GC. To utilise the full spectrum of molecular information contained in a complex crude oil and resolved by GC×GC for the accurate establishment of oil similarities instead of relying on a relatively small number of biomarkers, Ventura and coworkers used multiway principal component analysis (MPCA). MPCA in this application quantitatively compares every compound eluting within the same first- and second-dimension RT with eluents in that same GC×GC space in other fluids. The comparison based on GC×GC chromatograms included 3500 and more quantified components. Furthermore, three individual regions were identified by Ventura *et al.* that are suitable to analyse, resolve, and evaluate compositional changes related to the source organic matter of the hydrocarbons and their exposure to biological and physical weathering.

MPCA was demonstrated to be an effective tool to resolve multimolecular differences, even between very similar fluids, as well as to evaluate the degree of molecular relatedness and group oils into families. It was possible to quantitatively determine compositional and instrumental artefacts in order to exclude their impact on the establishment of similarities and differences.

Contaminants (*e.g.* alkenes introduced from drilling fluids) could be identified using factor loading plots and did not disturb the evaluation of the degree of the fluids' relatedness.

In order to identify minute differences in otherwise very similar oils, high-resolution techniques like GC×GC are required. Powerful data mining methods such as MPCA are needed to extract the unique molecular differences from the large data sets obtained from GC×GC, making GC×GC-MPCA a valuable combination to study reservoir connectivity, or discriminate between unique molecular compositions derived from source-dependent or weathering-related processes.

12.4.1.3 Identification and Quantification of Contaminants in Crude Oil

Drilling fluids play an essential role in the drilling process. However, they are dreaded by geochemists because they can significantly contaminate valuable samples, both fluid samples and sediment samples, essentially rendering them useless. Companies lose valuable information required to understand the reservoir, thermal maturity, the source of the petroleum hydrocarbons, and source rock quality in the drilled section which in the long term cause significant financial losses. Oil-based drilling fluids contain compounds that are equally present in the reservoir fluid, thus contamination with synthetic oil-based muds such as linear α-olefins (LAOs) or internal olefins (IOs) irreversibly alter the sample and prevent analysis of the indigenous oil composition.

Because of the complexity of crude oils, recognition and moreover quantification of IOs and LAOs can be challenging using 1D GC techniques. Reddy *et al.*[78] applied GC×GC-FID to identify and quantify alkene-based drilling fluids in crude oils, allowing them to eliminate the compounds that are derived from drilling fluids from the molecular composition of the crude oil.

As described in section 12.2.6, alkenes are separated from the range of n-alkanes in second dimension on a non-polar/polar column combination. Hence, the presence of artificially introduced alkenes can be detected and quantified in a GC×GC analysis down to an estimated 1% of contamination in crude oil.[78] This method is valuable to the industry as it enables detailed and accurate biomarker analysis of contaminated fluids and can also be used to monitor areas near wells for possible leaks or discharge into the environment.

Recently, Aeppli *et al.*[42] reported the use of olefins commonly found in synthetic drilling fluids to determine the source of oil sheens sampled in 2012 near the *Deepwater Horizon* site. Application of GC×GC-FID and GC×GC-TOF-MS allowed clear identification of three olefins in these oil sheen samples which clearly indicated that the oil sheens are sourced from leaking oil that was in contact or mixed with drilling fluid before release into the water. This observation ruled out the source of the sheens being the

coffer-dam oil, as was proposed by BP, because this oil does not contain any drilling fluid residues. Instead, presence of the olefins together with biomarker ratios and alkene ratios obtained from the highly resolved GC×GC-TOF-MS chromatograms suggest that the observed sheens originated from tanks and pits on the *Deepwater Horizon* wreckage.

These findings introduce a method to track drilling fluids released to the environment and further provide a framework for assessment of the fate of drilling fluids commonly released during exploration activities around the world.

12.4.2 Detailed Biomarker Analysis

12.4.2.1 Diamondoids

Diamondoids are very resistant to biodegradation[79] and are of particular interest to petroleum geochemists for thermal maturity assessment of highly mature oils.

With the use of GC×GC-TOF-MS, diamondoids could be effectively separated from normal and branched alkanes and other saturated hydrocarbons.[53–55] A large number of additional diamondoids could be separated and identified in addition to the diamondoids that were known to date using 1D GC. Wang *et al.*[54] recognised and identified over 100 individual substitutions of adamantane, diamantine, and triamantane. Silva *et al.*[55] identified tetramantanes and propyltriamantanes. These very recent studies present the start of a fruitful in depth discovery of diamondoids and their formation mechanisms.

12.4.2.2 Plant Markers

The GC×GC separation of angiosperm-derived saturated pentacyclic triterpenoids 18α(H)-, 18β(H)-oleanane and lupane was described by Eiserbeck *et al.*[56] The resolution of 18α(H)-oleanane and lupane using a similar column combination (non-polar/polar) was also reported by Silva *et al.*[20] The oleanane isomers and lupane coelute on a 1D GC system. Separation of all three of these compounds in one analysis could not be achieved previously. These compounds are very important angiosperm biomarkers for the recognition of terrigenous organic matter. However, the presence and abundance of individual plant biomarkers has not been well studied and understood in their information content, because of the challenges of separation. This applies not only to the three most commonly applied and well known angiosperm biomarkers—the oleanane isomers and lupine—but in particular to the amount of information that could be obtained from the detailed study of the distribution of the various diagenetic products of the biological precursors amyrin and betulin. GC×GC provides the tools to investigate the presence and abundances of the various compound classes present in one single sample that are derived from the same precursors and

can be studied in one single analysis, and direct comparison allows conclusions about the diagenetic processes within this biomarker class.

Eiserbeck *et al.*[27] extended the separation of plant biomarkers using GC×GC to these various compound classes. Only one whole-oil/source rock extract analysis was required to achieve baseline separation of commonly low abundant higher plant biomarkers such as the saturated C_{24} des-A- and C_{23} nor-des-A-compounds series including lupanoids, oleanoids, and ursanoids and their mono- and diunsaturated homologues.[27] A clear elution pattern for each series could be displayed (see section 12.2.6) with the series eluting parallel to each other, shifted in first- and second-dimension retention time (Figure 12.12).

Furthermore, components with identical molecular masses and fragmentation patterns were resolved in the second GC dimension, for instance tentatively identified des-A-lupane and nor-des-A-ursane/taraxastane (Figure 12.12a), or the coelution of des-A-lupene and des-A-lupadiene with two isomers, respectively (Figure 12.12b). These compounds could not be identified or quantified using 1D GC techniques.

GC×GC-TOF-MS is particularly valuable for separation problems of coeluting components with identical molecular masses and fragmentation pattern because the mass spectral similarity prevents separation based on extracted ion chromatograms or even metastable transition monitoring 1D GC systems.

Additional critical 1D GC separation problems in studies of angiosperm biomarkers that were resolved by GC×GC in second-dimension separation include the coelution of 24-norlupane and norhopane as well as 24,28-bisnorlupane and bisnorhopane (Figure 12.13), monoaromatic des-A-compounds ($M^+ = 310$), and triaromatic pentacyclic triterpenoids ($M^+ = 342$) (Figure 12.12c).

Taraxastane, another biomarker indicating land-plant input to the source organic matter,[80] was reported to elute later in the first and second dimension than α,β-hopane, moretane and oleanane.[27] The 25-norhopane series in biodegraded samples elutes earlier in the second dimension and thus does not coelute with higher-plant-derived saturated C_{28}- and C_{29}-compounds.

Many more compounds could be identified due to the sensitivity and resolution of GC×GC than were detected by traditional 1D GC, including isomers of known compounds as well as potentially new biomarkers. Some unsaturated triterpenoids are thermally unstable and prone to rearrangement. Taraxer-14-ene, for instance, coelutes in traditional GC-MS analysis with n-C_{30} alkane. Molecular sieving procedures[81] to separate these compounds before the analysis activate rearrangement of taraxer-14-ene to a mixture of oleanene isomers.[82] The increased resolution and sensitivity of GC×GC-TOF-MS enables the separation of such unstable compounds in a whole-oil analysis without loss in resolution maintaining the natural distribution of biomarkers in the sample.

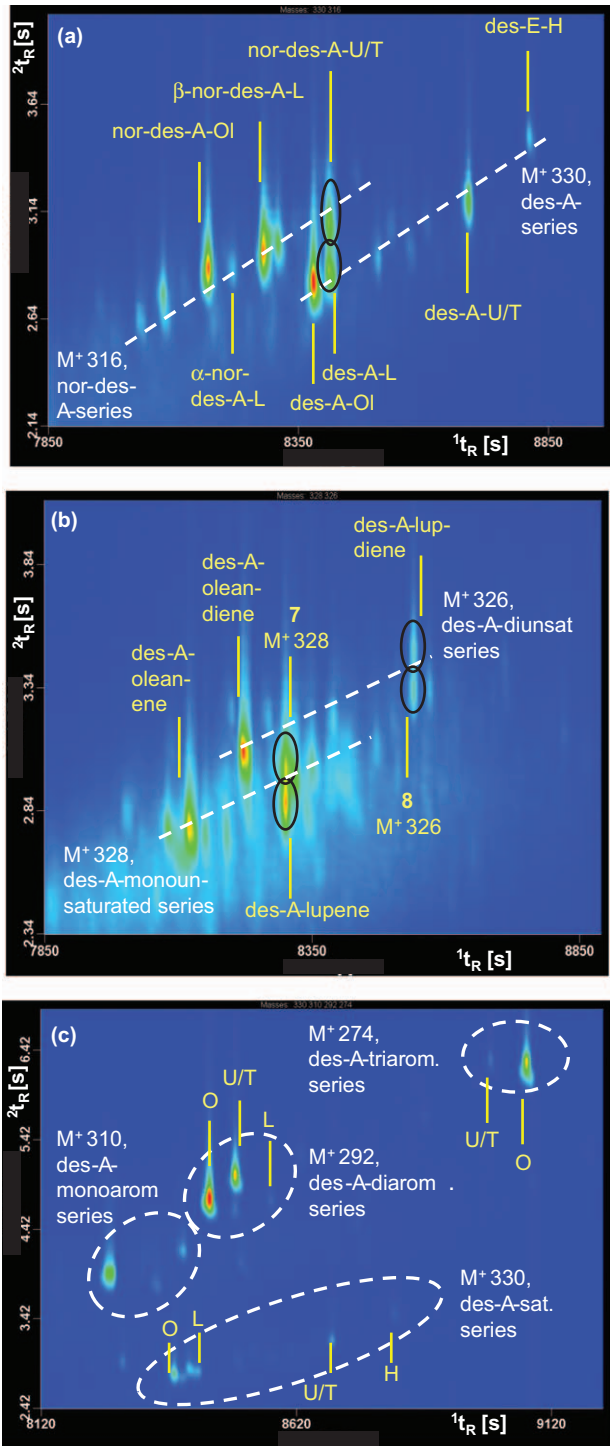

12.4.3 Unresolved Complex Mixtures

UCMs present challenges for the identification and quantification of resolved compounds using traditional GC-MS. Furthermore, the thousands of unresolved compounds within the UCM contain valuable information about the organic matter and also can contribute to the understanding of biodegradation processes. The high resolving power of GC×GC was applied to study non-degraded compounds in biodegraded samples as well as the composition of the UCM itself.

Many studies have been published on the successful application of GC×GC to questions related to degraded fluids.[14,17,23,27,83] Tran *et al.*[14] investigated the chemical composition of UCMs in three sets of oils from Australia, each set representing one oil family, and each sample within one set was exposed to a different level of biodegradation. The three sets were from marine, land-plant, and mixed marine and land-plant-derived organic matter, respectively. Chemical changes with progressing biodegradation were observed for each type of organic matter. A polar/non-polar column configuration was applied based on the suggestion that UCM is dominated by aliphatic, non-polar compounds,[17,84] which was confirmed by the position of the bulk of the UCM within the chromatographic plane. Tran *et al.*[14] showed that the different sources of the oils had little impact on the composition of the UCM. In all three oil families, the main compound class resolved from the UCM with GC×GC was C_1–C_7 alkyl-decahydronaphthalenes (alkyl-decalin). The dominating alkyl substitutions shift with increasing degree of biodegradation, from C_1–C_3-substituted isomers dominating oils exhibiting lower levels of degradation to C_4–C_7 isomers, which are more abundant in highly degraded oils. The longer the alkyl chain, the more isomers were observed in the GC×GC chromatogram, eluting in a parallel bands across the chromatographic plane. It was proposed that the coelution of both the isomers within one band as well as the bands with each other accounts for the UCM 'hump' in traditional 1D GC chromatograms. Alkyl-decalins were observed as constituents of UCM derived from biodegradation before, using GC×GC analysis,[17,23,49,52] *e.g.* in intertidal sediments contaminated with residual hydrocarbons after oil spills,[49] although less obvious due to the use of the more common

Figure 12.12 GC×GC-TOFMS ion chromatograms illustrating elution order and separation results for tetracyclic triterpenoids in oil C2. (a) Extracted ion chromatogram *m/z* 330 + 316. (b) Extracted ion chromatogram *m/z* 328 + 326. (c) Extracted ion chromatogram *m/z* 330 + 310 + 292 + 274 representing saturated, mono-, di- and triaromatic tetracyclic triterpenoids. O, oleanane; U/T, ursane/taraxastanes; L, lupine; H, hopane. Dashed lines represent the location of the series. Des-A-compounds were tentatively identified *via* comparison of GC-MS, GC-MRM-MS, and GC×GC-TOF chromatograms and mass spectra with elution orders and mass spectra reported in the literature.
Reprinted from Eiserbeck *et al.*,[27] Copyright (2012), with permission from Elsevier.

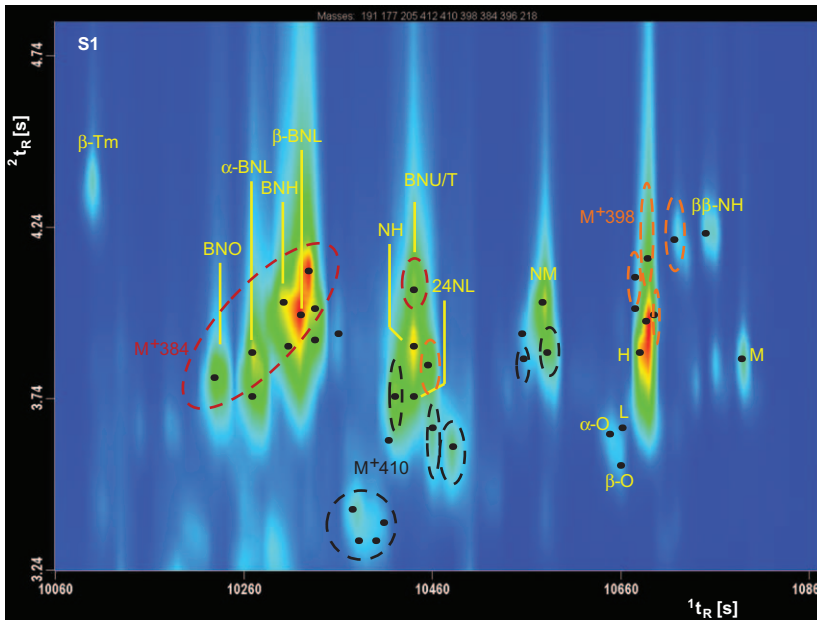

Figure 12.13 Section of the combined GC×GC-TOFMS EIC of the masses *m/z* 191, 177, 205, 412, 410, 398, 396, 384, 218 of rock extract S1. Key: dashed circles indicate groups of compounds (especially unidentified compounds based on the same molecular mass. Red: $M^+ = 384$, orange; $M^+ = 398$, black; $M^+ = 410$. β-Tm, 22,29,30-trinor-17β-hopane; α-BNL, 17α-24,28-bisnorlupane; β-BNL, 17β-24,28-bisnorlupane; BNH, 28,30-bisnorhopane; BNO, tentatively identified as 24,28-bisnoroleanane; NH, 30-norhopane; BNU/T, tentatively identified as 24,28-bisnorursane/taraxastane; 24NL, 24-norlupane; NM, 30-normoretane; H, 17α,21β(H)-hopane; α-O, 18α(H)-oleanane; β-O, 18β(H)-oleanane; L, lupine; ββ-NH, 17β,21β(H)-30-norhopane; M, moretane.
Reprinted from Eiserbeck *et al.*,[27] Copyright (2012), with permission from Elsevier.

non-polar/polar column configuration in these earlier studies. The polar/non-polar column configuration used by Tran *et al.*[14] was considered preferable to the more commonly used non-polar/polar combination to study the composition of UCM.

Although microbial biodegradation as the source of UCMs is more commonly studied and better understood, UCMs can also occur in systems that have been hydrothermally altered.[85–88]

Attempts to identify the constituents of UCMs in the past have been very involved and had varying success. Even extensive application of chemical degradation methods and use of capillary GC columns could not resolve some complex mixtures. The nature of the compounds that form the UCM remains unclear.

Ventura *et al.*[23] analysed samples from the Archaean which exposed varying degrees and topologies of UCMs that were irresolvable by traditional GC-MS. The researchers applied the increased separation power of GC×GC to facilitate tentative identification of a range of compound classes that were embedded within these UCM types. Based on the topology of the UCMs derived from 1D GC and the chemical composition derived from GC×GC analysis, they were able to characterise three different types of UCM in their sample set.

Type I UCM had the majority of the UCM in the lower molecular weight region and contained a range of mono- to hexacycloalkanes of unknown origin. Type II was characterised by a UCM of higher molecular weight and contained mostly C_{35}–C_{40} archaeal lipids. Type III represents a mix of type I and type II UCMs. This study demonstrated that GC×GC analysis of UCM in archaeal samples can provide valuable information about the biological source and diagenetic history of the organic matter. Furthermore, the analysis revealed that the samples from the Porcupine Gold Camp (northern Ontario, Canada)were unlikely to be derived from selective preservation of bioresistant compounds as it occurs during biodegradation because easily biodegradable compounds such as n-alkanes and acyclic isoprenoids were abundant in all samples. Very low concentrations of 25-norhopanes and the presence of highly isomerised archaeal lipids observed in type II UCM and the high abundance of mono- to hexacycloalkanes in type I UCM cannot be explained by biodegradation as source of the UCM, but rather suggest hydrothermal alteration as the likely degradation process. Type II UCM was proposed to result from the diagenetic alteration of biogenic material *via* a coupled process of isomerisation caused by hydrothermal stress in presence of high hydrogen pressure (hydrothermal conditions) and hydrocarbon cracking.

These insights support the study of the effects of hydrothermal alteration on the composition and preservation of Archaean organic matter and thus can help to determine the diversity of geological localities bearing extractable hydrocarbons.

In 2012, Ventura *et al.*[83] further investigated the genesis and evolution of hydrothermal petroleum, again utilising the power of GC×GC coupled with statistical partial least squares (PLS) linear regression analysis. Two simple metrics were introduced to quantitatively determine the alteration of maltene fractions in simple and complex mixtures and UCMs within GC×GC data. A molecular complexity metric quantifies the chromatographic complexity of a GC-amenable hydrocarbon fluid. The second metric is PLS linear regression of RT of individual compounds in petroleum. These two proxies were found to constrain the geochemical parameters that lead to structural ordering of the UCM in a GC×GC chromatogram. The authors compared samples collected from different stratigraphic or geographic hydrothermal environments employing the above metrics, as well as subtracted GC×GC chromatograms, which identified a characteristic multimolecular pattern of high molecular weight PAH migration.

The results showed evidence that, unlike the UCM derived from biodegradation which is characterised by an intensified baseline due to the degradation of n-alkanes, the UCMs in hydrothermal petroleum are a unique assemblage of biomarkers dominating the hydrocarbon composition. They take shape in a continuous series of compounds across compound classes. The structural ordering of the UCM that resulted from the composition of the source organic matter coupled with the degree of thermal alteration of the oil was only visible in a GC×GC chromatogram. The study concluded that UCMs from hydrothermal alteration/oxidative weathering appear to represent the early stages of hydrothermal petroleum formation. Continued pyrolysis and oxidation reduces hydrocarbon complexity as a result of extensive dehydrogenation and dealkylation.

12.4.4 Depositional Environments

Oliveira *et al.*[34,35] recognised the presence of onoceranes as a possible additional proxy for depositional paleoenvironments. With the use of GC×GC-TOF-MS, the researchers identified a series of onocerane isomers in representative oil samples from the Potiguar Basin and Cumuruxatiba Basin in Brazil. Both oil families are the result of multiple charge events, combining characteristics of an older charge which was subsequently biodegraded, and a younger non-biodegraded charge. Based on biomarker parameters the depositional environments of these oils could be classified as lacustrine and marine. With the use of GC×GC-TOF-MS, it was identified that the lacustrine samples contained two distinct series of 3β-methylhopane and onocerane isomers, respectively, whereas the marine samples exhibited a predominance of the 2α-methylhopane series and lack of onocerane isomers. The results suggest that the presence of an onocerane series might be a proxy for lacustrine depositional paleoenvironments.

12.5 Limitations

A critical part in the comprehensive 2D GC is the modulator which traps, focuses, and releases preseparated compound packages onto the secondary column. Improvements in the modulation times could increase the resolution power of GC×GC, as indicated by Blumberg *et al.*[89]

Further expansion in the application of GC×GC could be achieved by technical developments in acquisition rates of detectors such as quadrupole MS or irMS in order to couple the full separation power of GC×GC with a broader variety of detectors. A combination of the resolution of GC×GC coupled to irMS is particularly desirable because compound-specific isotope analysis (CSIA) requires baseline separation of the compounds, which is often a very challenging or even unachievable task and currently requires numerous wet chemical separation steps.

However, the biggest challenge in the application of GC×GC to date is the handling of the overwhelming amount of data produced by this technique.

More advanced data processing and data mining software and techniques are required to fully utilise the data provided in a GC×GC analysis. To date, information reduction in form of extracted ion chromatograms is often applied to reduce the available amount of data to a level we humans can comprehend, still neglecting the full picture that is presented to us in a GC×GC chromatogram.

12.6 Summary and Future of GC×GC

GC×GC-TOF-MS will become a platform technology dedicated specifically to energy, environment, and earth science research. Its various applications will not be limited to petroleum, but will also be extended to mineral exploration, evolution of our planet's history, and tracing contaminants in our environment. GC×GC-TOF-MS will support research from a very broad range of disciplines in the areas of oil and mineral exploration, human and coastal impacts on our environment, potable water supplies, climate, and paleoclimate change.

Acknowledgements

CMR would like to thank the GOMRI DEEP-C consortium for support.

References

1. Z. Liu and J. B. Phillips, *J. Chromatogr. Sci.*, 1991, **29**, 227–231.
2. M. Adahchour, J. Beens, R. J. J. Vreuls and U. A. T. Brinkman, *Trends Anal. Chem.*, 2006, **25**, 438–454.
3. M. Adahchour, J. Beens, R. J. J. Vreuls and U. A. T. Brinkman, *Trends Anal. Chem.*, 2006, **25**, 540–553.
4. M. Adahchour, J. Beens, R. J. J. Vreuls and U. A. T. Brinkman, *Trends Anal. Chem.*, 2006, **25**, 821–840.
5. M. Adahchour, J. Beens, R. J. J. Vreuls and U. A. T. Brinkman, *Trends Anal. Chem.*, 2006, **25**, 726–741.
6. M. Adahchour, J. Beens and U. A. T. Brinkman, *J. Chromatogr. A*, 2008, **1186**, 67–108.
7. J. B. Phillips and J. Beens, *J. Chromatogr. A*, 1999, **856**, 331–347.
8. J. Beens and U. A. T. Brinkman, *Trends Anal. Chem.*, 2000, **19**, 260–275.
9. E. B. Ledford, C. A. Billesbach and Q. Y. Zhu, *J. High Resolut. Chromatogr.*, 2000, **23**, 205–207.
10. P. J. Marriott, S.-T. Chin, B. Maikhunthod, H.-G. Schmarr and S. Bieri, *Trends Anal. Chem.*, 2012, **34**, 1–21.
11. J. V. Seeley, in *Gas Chromatography*, Elsevier, Amsterdam, 2012, pp. 161–185.
12. J. S. Arey, R. K. Nelson, L. Xu and C. M. Reddy, *Anal. Chem.*, 2005, **77**, 7172–7182.
13. J. M. D. Dimandja, *Anal. Chem.*, 2004, **76**, 167A–174A.

14. T. C. Tran, G. A. Logan, E. Grosjean, D. Ryan and P. J. Marriott, *Geochim. Cosmochim. Acta*, 2010, **74**, 6468–6484.
15. G. T. Ventura, F. Kenig, C. M. Reddy, J. Schieber, G. S. Frysinger, R. K. Nelson, E. Dinel, R. B. Gaines and P. Schaeffer, *Proc. Natl Acad. Sci. U. S. A.*, 2007, **104**, 14260–14265.
16. R. B. Gaines, G. S. Frysinger, M. S. Hendrick-Smith and J. D. Stuart, *Environ. Sci. Technol.*, 1999, **33**, 2106–2112.
17. G. S. Frysinger, R. B. Gaines, L. Xu and C. M. Reddy, *Environ. Sci. Technol.*, 2003, **37**, 1653–1662.
18. A. Aguiar, A. I. Silva Júnior, D. A. Azevedo and F. R. Aquino Neto, *Fuel*, 2010, **89**, 2760–2768.
19. G. S. Frysinger and R. B. Gaines, *J. Sep. Sci.*, 2001, **24**, 87–96.
20. R. S. F. Silva, H. G. M. Aguiar, M. D. Rangel, D. A. Azevedo and F. R. Aquino Neto, *Fuel*, 2011, **90**, 2694–2699.
21. T. C. Tran, G. A. Logan, E. Grosjean, J. Harynuk, D. Ryan and P. Marriott, *Org. Geochem.*, 2006, **37**, 1190–1194.
22. G. T. Ventura, G. J. Hall, R. K. Nelson, G. S. Frysinger, B. Raghuraman, A. E. Pomerantz, O. C. Mullins and C. M. Reddy, *J. Chromatogr. A*, 2011, **1218**, 2584–2592.
23. G. T. Ventura, F. Kenig, C. M. Reddy, G. S. Frysinger, R. K. Nelson, B. V. Mooy and R. B. Gaines, *Org. Geochem.*, 2008, **39**, 846–867.
24. G. T. Ventura, B. Raghuraman, R. K. Nelson, O. C. Mullins and C. M. Reddy, *Org. Geochem.*, 2010, **41**, 1026–1035.
25. F. C. Y. Wang and C. C. Walters, *Anal. Chem.*, 2007, **79**, 5642–5650.
26. M. Li, S. Zhang, C. Jiang, G. Zhu, M. Fowler, S. Achal, M. Milovic, R. Robinson and S. Larter, *Org. Geochem.*, 2008, **39**, 1144–1149.
27. C. Eiserbeck, R. K. Nelson, K. Grice, J. Curiale and C. M. Reddy, *Geochim. Cosmochim. Acta*, 2012, **87**, 299–322.
28. J. B. Phillips and J. Xu, *J. Chromatogr. A*, 1995, **703**, 327–334.
29. B. M. F. Ávila, A. Aguiar, A. O. Gomes and D. A. Azevedo, *Org. Geochem.*, 2010, **41**, 863–866.
30. B. M. F. Ávila, R. Pereira, A. O. Gomes and D. A. Azevedo, *J. Chromatogr. A*, 2011, **1218**, 3208–3216.
31. T. Dutriez, M. Courtiade, J. Ponthus, D. Thiébaut, H. Dulot and M.-C. Hennion, *Fuel*, 2012, **96**, 108–119.
32. T. Dutriez, D. Thiébaut, M. Courtiade, H. Dulot, F. Bertoncini and M.-C. Hennion, *Fuel*, 2013, **104**, 583–592.
33. L. S. Freitas, C. Von Mühlen, J. H. Bortoluzzi, C. A. Zini, M. Fortuny, C. Dariva, R. C. C. Coutinho, A. F. Santos and E. B. Caramão, *J. Chromatogr. A*, 2009, **1216**, 2860–2865.
34. C. R. Oliveira, A. A. Ferreira, C. J. F. Oliveira, D. A. Azevedo, E. V. Santos Neto and F. R. Aquino Neto, *Org. Geochem.*, 2012, **46**, 154–164.
35. C. R. Oliveira, C. J. F. Oliveira, A. A. Ferreira, D. A. Azevedo and F. R. Aquino Neto, *Org. Geochem.*, 2012, **53**, 131–136.
36. A. M. Booth, A. G. Scarlett, C. A. Lewis, S. T. Belt and S. J. Rowland, *Environ. Sci. Technol.*, 2008, **42**, 8122–8126.

37. M. F. Almstetter, I. J. Appel, M. A. Gruber, C. Lottaz, B. Timischl, R. Spang, K. Dettmer and P. J. Oefner, *Anal. Chem.*, 2009.
38. G. Saravanabhavan, A. Helferty, P. V. Hodson and R. S. Brown, *J. Chromatogr. A*, 2007, **1156**, 124–133.
39. C. A. Bruckner, B. J. Prazen and R. E. Synovec, *Anal. Chem.*, 1998, **70**, 2796–2804.
40. L. Xie, P. J. Marriott and M. Adams, *Anal. Chim. Acta*, 2003, **500**, 211–222.
41. T. Gröger, M. Schäffer, M. Pütz, B. Ahrens, K. Drew, M. Eschner and R. Zimmermann, *J. Chromatogr. A*, 2008, **1200**, 8–16.
42. C. Aeppli, C. A. Carmichael, R. K. Nelson, K. L. Lemkau, W. M. Graham, M. C. Redmond, D. L. Valentine and C. M. Reddy, *Environ. Sci. Technol.*, 2012, **46**, 8799–8807.
43. J. S. Arey, R. K. Nelson, D. L. Plata and C. M. Reddy, *Environ. Sci. Technol.*, 2007, **41**, 5747–5755.
44. J. S. Arey, R. K. Nelson and C. M. Reddy, *Environ. Sci. Technol.*, 2007, **41**, 5738–5746.
45. J. A. DeMello, C. A. Carmichael, E. E. Peacock, R. K. Nelson, J. Samuel Arey and C. M. Reddy, *Marine Pollution Bulletin*, 2007, **54**, 894–904.
46. C. Farwell, C. M. Reddy, E. Peacock, R. K. Nelson, L. Washburn and D. L. Valentine, *Environ. Sci. Technol.*, 2009, **43**, 3542–3548.
47. K. L. Lemkau, E. E. Peacock, R. K. Nelson, G. T. Ventura, J. L. Kovecses and C. M. Reddy, *Mar. Pollut. Bull.*, 2010, **60**, 2123–2129.
48. R. K. Nelson, B. M. Kile, D. L. Plata, S. P. Sylva, L. Xu, C. M. Reddy, R. B. Gaines, G. S. Frysinger and S. E. Reichenbach, *Environ. Forensics*, 2006, **7**, 33–44.
49. E. E. Peacock, G. R. Hampson, R. K. Nelson, L. Xu, G. S. Frysinger, R. B. Gaines, J. W. Farrington, B. W. Tripp and C. M. Reddy, *Mar. Pollut. Bull.*, 2007, **54**, 214–225.
50. C. M. Reddy, J. S. Arey, J. S. Seewald, S. P. Sylva, K. L. Lemkau, R. K. Nelson, C. A. Carmichael, C. P. McIntyre, J. Fenwick, G. T. Ventura, B. A. S. Van Mooy and R. Camilli, *Proc. Natl Acad. Sci. U. S. A.*, 2012, **109**, 20229–20234.
51. G. D. Wardlaw, J. S. Arey, C. M. Reddy, R. K. Nelson, G. T. Ventura and D. L. Valentine, *Environ. Sci. Technol.*, 2008, **42**, 7166–7173.
52. R. B. Gaines, G. S. Frysinger, C. M. Reddy and R. K. Nelson, in *Spill Oil Fingerprinting and Source Identification*, ed. Z. Wang and S. Stout, Academic Press, New York, 2006, pp. 169–202.
53. S. Li, S. Hu, J. Cao, M. Wu and D. Zhang, *Int. J. Mol. Sci.*, 2012, **13**, 11399–11410.
54. G. Wang, S. Shi, P. Wang and T. G. Wang, *Fuel*, 2013, **107**, 706–714.
55. R. C. Silva, R. S. F. Silva, E. V. R. de Castro, K. E. Peters and D. A. Azevedo, *Fuel*, 2013, **112**, 125–133.
56. C. Eiserbeck, R. K. Nelson, K. Grice, J. Curiale, C. M. Reddy and P. Raiteri, *J. Chromatogr. A*, 2011, **1218**, 5549–5553.
57. A. L. Payeur, P. A. Meyers and R. D. Sacks, *Org. Geochem.*, 2011, **42**, 1263–1270.

58. C. von Mühlen, E. C. de Oliveira, P. D. Morrison, C. A. Zini, E. B. Caramao and P. J. Marriott, *J. Sep. Sci.*, 2007, **30**, 3223–3232.
59. C. von Mühlen, E. C. de Oliveira, C. A. Zini, E. B. Caramão and P. J. Marriott, *Energy Fuels*, 2010, **24**, 3572–3580.
60. C. Flego and C. Zannoni, *Fuel*, 2011, **90**, 2863–2869.
61. P. M. Harvey and R. A. Shellie, *J. Chromatogr. A*, 2011, **1218**, 3153–3158.
62. R. Shellie, P. Marriott, M. Leus, J.-P. Dufour, L. Mondello, G. Dugo, K. Sun, B. Winniford, J. Griffith and J. Luong, *J. Chromatogr. A*, 2003, **1019**, 273–278.
63. R. A. Shellie, L.-L. Xie and P. J. Marriott, *J. Chromatogr. A*, 2002, **968**, 161–170.
64. G. Purcaro, P. Quinto Tranchida, L. Conte, A. Obiedzińska, P. Dugo, G. Dugo and L. Mondello, *J. Sep. Sci.*, 2011, **34**, 2411–2417.
65. G. Purcaro, P. Q. Tranchida, C. Ragonese, L. Conte, P. Dugo, G. Dugo and L. Mondello, *Anal. Chem.*, 2010, **82**, 8583–8590.
66. D. Valentine, C. Reddy, C. Farwell, T. Hill, O. Pizarro, D. Yoerger, R. Camilli, R. Nelson, E. Peacock, S. Bagby, B. Clarke, C. Roman and M. Soloway, *Nat. Geosci.*, 2010, **3**, 345–348.
67. C. Eiserbeck, PhD, Curtin University, 2011.
68. K. E. Peters, C. C. Walters and J. M. Moldowan, *The Biomarker Guide, Volume 2: Biomarkers and Isotopes in Petroleum Exploration and Earth History*, Cambridge University Press, Cambridge, 2005.
69. N. Varotsis and P. Guieze, *J. Petrol. Sci. Eng.*, 1996, **15**, 81–89.
70. H. P. Roenningsen, I. Skjevrak and E. Osjord, *Energy Fuels*, 1989, **3**, 744–755.
71. C. A. Carmichael, J. S. Arey, W. M. Graham, L. J. Linn, K. L. Lemkau, R. K. Nelson and C. M. Reddy, *Environ. Res. Lett.*, 2012, **7**.
72. R. P. Rodgers, A. M. McKenna, R. K. Nelson, W. K. Robbins, C. S. Hsu, C. M. Reddy and A. G. Marshall, *Abstr. Papers Am. Chem. Soc.*, 2011, **241**.
73. H. K. White, P.-Y. Hsing, W. Cho, T. M. Shank, E. E. Cordes, A. M. Quattrini, R. K. Nelson, R. Camilli, A. W. J. Demopoulos, C. R. German, J. M. Brooks, H. H. Roberts, W. Shedd, C. M. Reddy and C. R. Fisher, *Proc. Nat.l Acad. Sci. U. S. A.*, 2012, **109**, 20303–20308.
74. J. P. Ryan, Y. Zhang, H. Thomas, E. V. Rienecker, R. K. Nelson and S. R. Cummings in *Monitoring and Modeling the Deepwater Horizon Oil Spill: A Record-Breaking Enterprise*, ed. Y. Liu, A. MacFadyen, Z. G. Ji and R. H. Weisberg, 2011, vol. 195, 63–75.
75. *On Scene Coordinator Report, Deepwater Horizon Oil Spill*, U.S. Coast Guard, 2011.
76. R. C. Prince, D. L. Elmendorf, J. R. Lute, C. S. Hsu, C. E. Haith, J. D. Senius, G. J. Dechert, G. S. Douglas and E. L. Butler, *Environ. Sci. Technol.*, 1994, **38**, 142–145.
77. R. Camilli, C. M. Reddy, D. R. Yoerger, B. A. S. Van Mooy, M. V. Jakuba, J. C. Kinsey, C. P. McIntyre, S. P. Sylva and J. V. Maloney, *Science*, 2010, **330**, 201–204.

78. C. M. Reddy, R. K. Nelson, S. P. Sylva, L. Xu, E. A. Peacock, B. Raghuraman and O. C. Mullins, *J. Chromatogr. A*, 2007, **1148**, 100–107.
79. K. Grice, R. Alexander and R. I. Kagi, *Org. Geochem.*, 2000, **31**, 67–73.
80. H. P. Nytoft, G. Kildahl-Andersen and O. J. Samuel, *Org. Geochem.*, 2010, **41**, 1104–1118.
81. K. Grice, R. d. Mesmay, A. Glucina and S. Wang, *Org. Geochem.*, 2008, **39**, 284–288.
82. J. Rullkötter, T. M. Peakman and H. L. Ten Haven, *Org. Geochem.*, 1994, **21**, 215–233.
83. G. T. Ventura, B. R. T. Simoneit, R. K. Nelson and C. M. Reddy, *Org. Geochem.*, 2012, **45**, 48–65.
84. S. D. Killops and M. A. H. A. Al-Juboori, *Org. Geochem.*, 1990, **15**, 147–160.
85. A. I. Rushdi and B. R. T. Simoneit, *Appl. Geochem.*, 2002, **17**, 1401–1428.
86. A. I. Rushdi and B. R. T. Simoneit, *Appl. Geochem.*, 2002, **17**, 1467–1494.
87. B. R. T. Simoneit, A. Y. Lein, V. I. Peresypkin and G. A. Osipov, *Geochim. Cosmochim. Acta*, 2004, **68**, 2275–2294.
88. P. F. Z.-d. Valle and B. R. T. Simoneit, *Appl. Geochem.*, 2005, **20**, 2343–2350.
89. L. M. Blumberg, F. David, M. S. Klee and P. Sandra, *J. Chromatogr. A*, 2008, **1188**, 2–16.